Problems of modeling radiation damage in crystals

V. M. Agranovich and V. V. Kirsanov

Institute of Spectroscopy, USSR Academy of Sciences, Krasnaya Pakhra (Moscow Oblast')
Usp. Fiz. Nauk **118**, 3–51 (January 1976)

Mathematical modeling of radiation defects in crystals is currently one of the fundamental methods of theoretical study of radiation damage. This review gives the fundamental results obtained in this field in the 15 years that have elapsed since the appearance of the pioneering study of Vineyard. The results are discussed of studying the structure of low- and high-energy cascades, the role of thermal lattice vibrations, the interaction of focusons and crowdions with lattice defects, the equlibrium structure of radiation defects, post-cascade distributions of radiation defects, and their influence on the mechanical properties of solids.

PACS numbers: 61.80.–x, 63.20.Mt

CONTENTS

"At first we valued the machine method only as on auxiliary tool for deriving exact analytical formulas. Unfortunately, it gradually became clear that our hopes bordered on hopelessness, while computer modeling of the processes proves to be the only approach within which one can encompass from a unified viewpoint the entire set of observed physical phenomena."

G. H. Vineyard[10]

1. INTRODUCTION

The vigorous growth of atomic energy, as well as the widespread development of studies in the field of thermonuclear fusion, causes radiation materials science to be one of the most important branches of modern solid state physics. Although extensive experimental material has accumulated in this field, the study of changes in the physical properties of solids under irradiation that arise from structural rearrangement (radiation damage) continues to present surprises. Phenomena have been discovered in the past 5–10 years and have begun to be intensively studied, such as radiation amorphization, radiation embrittlement, radiation swelling of non-fissioning metals and alloys, radiation hardening, radiation-stimulated diffusion, etc.

Experimental study in this field continues to develop. In line with the broader use of fast-neutron reactors that is planned for the future, especial interest falls on the study of the behavior of solids under high doses and fluxes of neutrons (up to 10^{16} neutrons/cm^2 sec). Yet the studies on the field of thermonuclear fusion render very topical the study of the effect on the properties of solids of fluxes of neutrons of higher energies ($E \approx 6$–14 MeV).

It is therefore natural that prediction of the behavior of materials under these conditions requires the construction of a sufficiently complete theory of radiation damage. Although this sort of theory began to develop even at the dawn of atomic energy, there is yet no perfected picture of the entire complex of physical phenomena in solids that arise when high fluxes of nuclear particles act on them. Perhaps this situation is due to the small number of currently existing experiments that are sufficiently clearcut and decisive.

However, it is not ruled out that the relatively slow development of the theory of radiation damage also stems from the attitude toward it on the part of theoretical physicists themselves. Thus, many of them often express doubts that the study of radiation damage could be a serious enough undertaking for them.[1)] However, considering the importance of the problems of radiation materials science, we can hardly agree with this viewpoint.

The first attempts at qualitative explanation of the

[1)]As a curiosity, we recall that an even more extreme viewpoint, as Peierls[135] has written, belongs to Pauli, who expressed an analogous doubt very long ago concerning studies in the field of solid-state theory in general.

processes that occur when a bombarding particle strikes a crystal were undertaken long ago, and we should note here first of all the study by Wigner in 1942. Yet the creation of an exact quantitative theory has faced an entire set of difficulties. The main one of these is that the investigator runs up against the many-body problem in trying to describe the development of radiation damage in a crystal.

A flux of bombarding particles striking a crystal and interacting with the atoms of the target gives rise to primary knock-on (displaced) atoms. The energy spectrum of the primary knock-on atoms and their spatial distribution are inhomogeneous, even when we bombard with monoenergetic particles. The primary knock-on atoms are inhomogeneously distributed in space and they have varying energies. They generate in the material cascades of atom-atom collisions that can differ sharply among themselves. Each cascade can contain up to several thousand simultaneously moving and interacting atoms. The probability is great that cascades and their individual branches will overlap, especially at high fluxes.

During its lifetime (of the order of 10^{-13}–10^{-14} sec), each cascade leaves behind it a set of the most varied defects, beginning with vacancies and interstitial atoms, and ending with complicated complexes of them. Each post-cascade ("embryonic") size and spatial distribution of defects tends in time to come to equilibrium with the surrounding crystal structure. Yet, under irradiation conditions, a new cascade can pass at any time through this unestablished distribution of defects, and its development can then differ markedly from the corresponding process in an ideal lattice. All of this is subject to the effect of the thermal lattice vibrations, mechanical stresses, electric fields, etc.

Attempts have been made to describe the various stages of development of radiation damage, and are still being made. Naturally, the possibilities are highly limited, in view of the factors cited above. The recent advent of computer modeling has proved more successful. Apparently this is precisely the approach to which we must currently tie our hopes of constructing a complete enough physical picture of radiation damage in solids.

While turning our main attention to the organization and results of computer modeling, we shall show below how its use permits one to obtain the qualitatively new regularities that are characteristic of ordered systems that consist of an enormous number of mutually interacting particles.

Depending on the methods being applied, computer models in radiation damage theory are classified as being causal, stochastic, or mixed. In the first case, one solves the equations of motion of a many-particle system. In the second, an element of chance is introduced into the calculational algorithm by the Monte Carlo method.

Actually, the fundamental study that founded the computer-modeling approach to radiation damage was one that was performed in the Brookhaven National Laboratory of the United States by Vineyard and his associates.[1] This study proposed the first computer model of the dynamics of radiation damage. At present, computer modeling has permeated all of the fundamental problems of radiation physics, and a rather broad range of physical phenomena has been studied with computer models.

In order to give a more or less complete general picture of the new results obtained here, we shall begin with the studies on the dynamics of radiation damage that directly border on Vineyard's approach (energy of the primary knock-on atom $E \leq 1$–2 keV; see Chaps. 2, 3). The structure of the cascades of atom-atom collisions has been analyzed within the framework of Vineyard's model and of a number of its generalizations (subdivision of the cascade into dynamic crowdions and focusons; ejection of interstitials to the periphery of the cascade; formation of an inner zone enriched in vacancies). An anisotropy of the threshold displacement energy has been found, and the effect on it has been studied of the thermal vibrations of the atoms (which proved to be highly important). The concept has been introduced of zones of spontaneous recombination of Frenkel' pairs, and an estimate has been given of their volumes. The collisions of dynamic crowdions and focusons with lattice defects has been studied, and a localization of cascades caused by thermal vibrations has been discovered.

The transition to treating the dynamics of radiation damage at higher energies of primary knock-on atoms ($E > 1$–2 keV) required a qualitative change in the procedure of machine modeling. More details on its features are given in Sec. C of Chap. 3. Yet here we shall only note that an analysis was conducted of the post-cascade defect structures (size distributions of different types of defects) within the framework of this approach, which essentially used the above-cited results of computer modeling of low-energy cascades, as depending on the energy of the primary knock-on atom.

Use of the computer-modeling method has made it possible to study complicated atomic configurations of lattice defects, and to determine also their most important characteristics: formation and binding energies, activation energy for displacement, etc. (see Chap. 4). One of the most important and interesting conclusions that one can draw from the results obtained here is the existence of a continuous evolution of defects, with increase in their dimensions and transformation into complete dislocation loops (of vacancy and interstitial types). Moreover, computer modeling has made it possible to treat also radiation annealing of the defect structures that arise upon irradiation, and thus to study the saturation of the relationships of altered crystal physical properties that are observed as one increases the radiation dose (see Chap. 5).

Of course, it is very interesting to be able to study not only the different types of defect structures that arise upon irradiation, but also their effect on the observable physical properties of crystals. It turns out (see Chap. 6) that the computer-modeling methods permit one here also to get a number of interesting results (e.g., to study the effect of defect distributions on the mobility of dislocations).

We should note that almost all of the results cited above were obtained with models that simulate cubic

metals. This is due to the relative simplicity of the form of the interatomic interaction in them. However, attempts have also been made to model the development of radiation damage in materials having a more complex interaction, in particular, in diatomic materials, and we shall take them up below.

The founding study by Vineyard and his associates[1] was published in 1960. In the 15 years that have elapsed, the line of study that arose has vigorously grown. The aim of this review is to illuminate the fundamental results that have been gained in the time that has elapsed.

Accordingly, we shall discuss in more detail in the following sections the different approaches to modeling various aspects and stages of development of radiation damage. We shall try to systematize the information that exists here, and in conclusion, we shall note the possible paths and prospectives of further studies. However, we shall begin with discussing one of the fundamental problems of constructing discrete models, namely, the problem of choosing the form of the interatomic interaction potential.

While taking account of the specifics of computer modeling, we shall be required at certain places in describing the methodology to represent the algorithms schematically in the form of very simple block diagrams and to use special terminology in individual cases. We hope here that this type of block diagrams will prove useful for readers who are interested not only in the currently existing physical results of machine modeling of radiation defects, but also in the methods of getting them.

Computer calculations with a designed and debugged algorithm recall in a certain sense experimental studies, so that it is with good reason that the term "computer experiment" has arisen recently. This involves the appearance in the text of the expressions "we observe," "we see," etc. Yet we would like to stress that in setting up a "computer experiment," just as in creating a new theory, not only imagination and physical intuition are important, but also knowing how to reject all second-rank factors. Computers are not yet omnipotent.

2. INTERATOMIC POTENTIALS

A very important feature of the methods of modeling radiation damage that are discussed here involves rejection both of describing them within the framework of elasticity theory and of using the so-called gas model. In modeling, one assumes, just as actually happens, that the atoms or ions in the solids form a crystal lattice of some type owing to mutual interaction, and its structure begins to break down as the primary knock-on atoms arise in the lattice. Since the development of radiation damage is a many-atom process, then in trying to model it on the microscopic level, the investigator first faces the need of possessing the interatomic potential in explicit form. Hence the problem of the interatomic interaction potential is one of the most important. In line with this, before we proceed to describing the potentials that are currently used, it seems pertinent to make some remarks concerning their choice. Of course, the chosen potential must correctly describe the actual interatomic interaction in the crystal over a very broad range of energies, since, e.g., in problems of the dynamics of radiation damage, the colliding atoms can have energies from zero up to several tens of kiloelectron volts. At the same time, the chosen potential must be represented by a rather simple function or by a not very unwieldy set of functions. Otherwise the computer will waste too much time on analyzing each interatomic interaction, so that the total time for analyzing all the interactions (e.g., ensembles of 500–10,000 atoms) will grow to such limits as to make the solution of the problem practically unattainable. We shall show below how different authors have tried to find the optimal solution.

We emphasize only that the representation of the potential energy of a system of atoms as a sum of pair interactions is only approximate. Yet the many-particle forces are not taken into account at all in the overwhelming majority of calculations. Systematic account taken of them and estimation of their role is involved in one of the unstudied problems of machine modeling of radiation defects (see below).

Figure 1 and Table 1 give in graphic and analytical forms some examples of interatomic pair potentials that are commonly used in modeling. For monatomic crystals, the most successful choice of potential seems to be that for α-iron (α-Fe), as carried out by Erginsoy, Vineyard, and Englert.[3] This potential is given in different forms for different distance ranges. For $r < 0.7\,l_0$ (l_0 is half of the cube edge in the body-centered cubic lattice), one uses the screened Coulomb potential

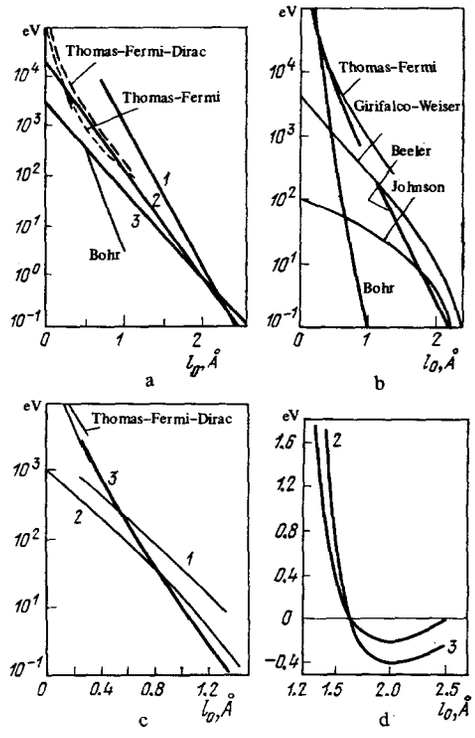

FIG. 1. The interatomic potentials used in modeling radiation damage (drawn in heavy lines and numbered). Abscissa—interatomic distance l_0 (Å), ordinate—energy V (eV). a) for copper,[1] b) for tungsten,[2] c, d) for α-iron ($l_0 = 1.43$ Å).[3,4]

TABLE 1. Interatomic interaction potentials.

Element	Distance range, A	Potential, eV
Iron I[5,6]	<2.40	$-2.195976\,(r^{-3.097910})^3+2.704060r^{-7.436448}$
	2.40—3.00	$-0.639230\,(r^{-3.115899})^3+0.477871r^{-1.881570}$
	3.00—3.44	$-1.115035\,(r^{-3.066403})^3+0.466892r^{-1.547967}$
	<2.40	$-4.719041\,(r^{-3.099035})^3-0.395690r^{+0.809049}$
Iron II[5]	2.40—3.00	$-0.886887\,(r^{-3.083289})^3+0.437641r^{-1.450695}$
	3.00—3.44	$-1.057432\,(r^{-3.069639})^3+0.434665r^{-1.441617}$
	<2.65	$-4.198744\,(r^{-3.017659})^3+0.607270r^{-2.518887}$
Tungsten[5]	2.65—3.32	$-0.235362\,(r^{-5.610045})^3+5.091237r^{-20.197978}$
	3.32—3.80	$-4.254329\,(r^{-3.446693})^3+1.593157r^{-5.806373}$
	2.00—2.53	$-1.496112\,(r^{-3.731397})^3-0.599656r^{-1.614190}$
Vanadium[7]	2.53—3.17	$0.095514\,(r^{-0.304062})^3-2.201314r^{-6.695125}$
	3.17—3.63	$-1.430039\,(r^{-3.361431})^3-0.309466r^{-1.095656}$

$$V(r)=\frac{0.7}{r}8573\exp(-6.547r). \quad (1)$$

In the range $0.7<r<1.35\,l_0$, the Born–Mayer potential was applied:

$$V(r)=8573\exp(-6.547r). \quad (2)$$

For $1.35<r<2.0$, the Morse potential was used:

$$V(r)=D\{\exp[-2\alpha(r-r')]-2\exp[-\alpha(r-r')]\}, \quad (3)$$

where $D=0.223$ eV, $\alpha=1.3885$ Å^{-1}, and $r'=2.845$ Å. In the range $2.0<r<2.5\,l_0$, one again uses a Morse potential, but multiplied by an arbitrarily chosen function of r that equals unity when $r=2\,l_0$, and smoothly declines to 0.1 when $r=2.5\,l_0$. For $r>2.5\,l_0$, the potential $V(r)$ was taken to be zero.

For small distances between the atoms, this composite potential (see Fig. 1) is repulsive in nature, but is weakly attractive at large distances. Comparison of the elastic moduli obtained experimentally and those calculated by using this potential gives quite satisfactory agreement (Table 2).

This potential satisfies the fundamental needs of the discrete model: when combined with small surface forces (see below concerning these), it gives a stable body-centered lattice having the correct lattice constants and the correct values of the first three elastic moduli. At small distances, it matches the Thomas–Fermi and Thomas–Dirac potentials. Moreover, it gives an acceptable threshold displacement energy.[3] In spite of the stated merits of this potential, one cannot model stable crystal lattices of certain types by using it.

In order to impart stability to the body-centered cubic lattice, the same Erginsoy, Vineyard, and Englert[3] were compelled in the machine modeling to apply to the two surface layers of atoms of the studied region of the crystal (the "microcrystallite") some forces small in modulus that simulate an additional attraction. Naturally, they thus sharply limited the potentialities of the model.[2)] This is because one must not "allow an approach" close to the boundaries of the "microcrystallite" in avoiding errors in the developing process (e.g., a cascade of atom-atom collisions). This requires that we make its volume larger than in the case that does not require introducing additional surface forces.

We note that situations can happen in some cases in the development of a cascade in which substantial overlap of the wave functions of more than two particles arises. Precisely in this case, the interaction energy is no longer represented by the sum of two-particle energies, but will contain terms in which the coordinates of three or more atoms prove to be involved (many-particle forces).

Unfortunately, attempts to include in computer models calculations of the interaction with allowance for many-particle forces face the as yet limited possibilities of modern computers. Even the most powerful computers spend an inadmissibly long time on these calculations (with account taken of their multiple iteration; see, e.g., [81]).

The choice of potentials that are suitable for modeling in diatomic crystals presents an even more complex problem. Here, too, only rather crude approximations are used. For example, the simple procedure proposed by Rimmer and Cottrell[9] is used for the case of the interaction potential of atoms of an inert gas with atoms of a metal. If one assumes that the interaction is central and pairwise, and that the metal–metal (E_M) and gas–gas (E_G) potentials are known, the metal–gas potential E_{M-G} is defined within the framework of this approximation as follows:

$$E_{M\text{-}G}(r)=\tfrac{1}{2}[E_M(2r_M)+E_G(2r_G)], \quad (4)$$

Here r_M is the "radius" of the metal atom, r_G is the "radius" of the gas atom, and $r=r_M+r_G$ is the distance between the centers of the metal and gas atoms.

For each given value of r, one seeks a pair of values of r_M and r_G that give the minimum value of the function (4). This minimum value of (4) is then taken as the metal–gas potential corresponding to the interatomic distance r. Since the potentials E_M and E_G themselves are complicated, even this simple procedure of Rimmer and Cottrell, which is repeated many times in analyzing the ensemble of interacting atoms, requires spending much computer time.

As the existing calculations have implied, a number of the important physical results of computer modeling fortunately vary little upon further refinement of the qualitatively correct (see above) pair potentials of the first approximation, in spite of the emphasized difficulties in choosing the atom-atom potentials. Apparently this arises from the large number of atoms in the cascade and in defect formation. Of course, refinement of the potentials remains necessary, and this

TABLE 2.

Elastic constants $\times 10^{11}$, dynes/cm^2	C_{11}	C_{12}	C_{14}	$B=(C_{11}+2C_{12})/3$
Experiment, $T\approx 0$°K	23.7	14.1	11.6	17.3
Calculation	19.2	16.4	10.4	17.3

[2)] In particular, it is precisely these limitations of the model that hinder machine modeling of the interesting physical processes that arise upon bombarding the surfaces of crystals with fluxes of fast ions. For a review of the corresponding effects, see[136, 137].

should stimulate further development of the theory of atom-atom interactions.

3. FEATURES OF THE DYNAMICS OF RADIATION DAMAGE IN CRYSTALS (FOCUSONS AND CROWDIONS, DEPLETED ZONES, ANISOTROPY OF THRESHOLD DISPLACEMENT ENERGIES AND SPONTANEOUS-ANNIHILATION ZONES)

In this chapter we shall treat models that simulate the rapidly occurring processes (with lifetimes of the order of 10^{-13} sec) that take place from the moment of onset of movement of the primary knock-on atom to the moment of cessation of the cascade of collisions, when the energy of the colliding atoms becomes comparable with the thermal energy. Upon being scattered by the lattice atoms, the bombarding particle can impart to them a kinetic energy whose size varies over a large range. For example, for neutron irradiation in reactors, the kinetic energy of the primary knock-on atom can lie in the range from 0 to several tens of kiloelectron volts. The development of the process here will depend on the region within this range in which the energy of the primary knock-on atom lies. In the small-energy region, such an atom will lose its energy on elastic collisions with other atoms. At large energies $E > E_{exc}$, the collisions become inelastic in nature, with the appearance of considerable electronic excitation up to the point of ionization.

Investigators usually concentrate especial attention on the elastic-collision region. This is to some extent justified, in that in most technically important cases of irradiation (e.g., irradiation in a reactor with neutrons of energies about 1 MeV), primary knock-on particles of energies $E < E_{exc}$ predominate in the energy spectrum of the recoil atoms. Yet, concerning the fate of primary knock-on atoms having energies in the inelastic-collision region, one assumes that these atoms lose energy in electronic excitations and ionization without causing structural changes in the lattice.

However, as we approach the energy boundary that separates elastic and inelastic collisions (e.g., $E_{exc} \approx 6$ keV for Cu[10]), they overlap with the primary knock-on atoms of the first region. Yet, even if we restrict the treatment to only the elastic-collision region, the energy range of the primary knock-on atoms still remains very broad. Along this line, one can try to introduce an energy threshold by classifying the cascades of collisions in the elastic region into high-energy (where the effect of the lattice is minimal) and low-energy cascades (where the crystal lattice exerts an appreciable influence). Estimates that have been performed with very simple models, e.g., by Thompson,[11] confirm that this classification is justified. We shall follow this classification, while remembering that it may be not needed at all when one uses powerful enough computers.

A. The Brookhaven method (Vineyard's model)

In 1960, Vineyard and his associates[1,12] proposed a model that permits one rather completely to study low-energy cascades of collisions in copper at the hypothetical absolute zero 0 °K (in the initial state, all the atoms of the ideal crystal lattice are at rest). The authors realized this model by using the most powerful computers then existing. Prior to the study by Vineyard and his associates, the theory of displacement of atoms in solids caused by fast particles had been developed by Harrison and Seitz,[13] Snyder and Neufeld,[14] Kinshin and Pease,[15] and others.

All these studies assumed that the cascade initiated by the primary knock-on atom is a sequence of independent atom-atom collisions, and that the initial positions of the colliding atoms are arbitrary. Thus, these studies took no account of the crystalline order of the atoms. However, here they introduced the concept that proved to be very important of a threshold energy for displacement of an atom from its site. The calculations of the number of displaced atoms that were performed under these assumptions generally turned out to agree poorly with the estimates that could be made from the experimental data (e.g., the discrepancy was as great as twentyfold in neutron bombardment[16]). It was natural to assume that these discrepancies involved the simplifications of the cascade models.

Several hypotheses were advanced in seeking a way out. While rejecting one of the hypotheses of the simple cascade theories, Seitz and Koehler[17] introduced the concept of a "temperature spike (peak)." They assume that upon collision, an entire macroscopic region of the lattice is perturbed, and is locally heated. Later these spikes were divided into two classes: 1) thermal spikes (whose excitation is so small that the atoms do not leave their lattice sites), and 2) displacement spikes (whose excitation is large enough that many atoms in the spike are displaced from the lattice sites). The peaks of Brinkman[18] belong to the latter class.

Having cast doubt on a second hypothesis of the cascade theories, Seeger[19] called attention to the fact that in metals a cascade can develop in such a way that many atoms are removed from the perturbed region by chains of displacements (dynamic crowdions) that propagate along the close-packed crystallographic directions. Then a zone is formed at the site of passage of the cascade that is quasiamorphous in nature, and in which the density of atoms can be much smaller than usual (Seeger depleted zones).

Although all these models are purely qualitative in nature, they correctly reflect individual details of the dynamics of radiation damage in crystals, and they clearly stress the defects of the simple cascade theories. All of this prepared the ground for creating a more exact quantitative description that proved possible only by using computers.

The essence of Vineyard's model consists in the following. One treats a finite region of a crystal (a "microcrystallite") around the initial site of the atom being displaced, in which the atoms interact by pairwise, central forces that correspond to potentials of the type, e.g., of the Born–Mayer potential. The bonding forces that arise from the conduction electrons (copper was treated in the first study[1]) were simulated by constant

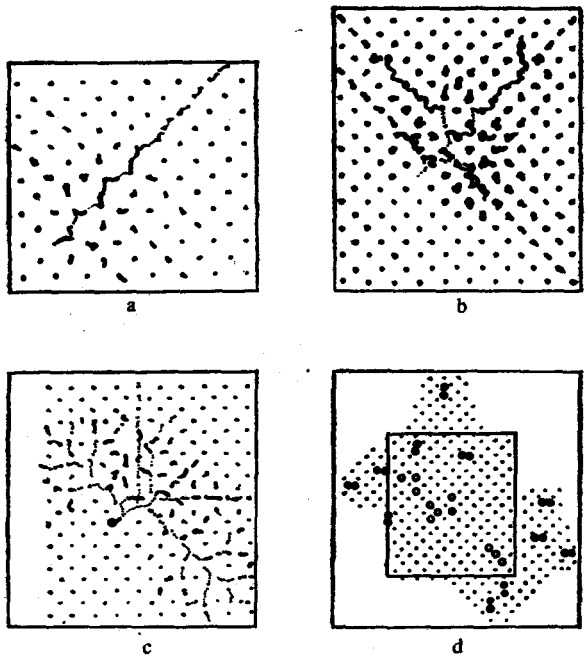

FIG. 2. Trajectories of the atoms participating in cascades of collisions in the f.c.c. crystal of copper (a–c) and the post-cascade structure (d).[1] ●—interstitial atoms; ○—vacancies. E_0 and θ_0 are the initial energy and angle of the primary knock-on atom; E_0 (eV): 50(a), 100(b), 400(c); $\theta_0 = 10°$ to [011].

forces applied to the boundary atoms that were directed into the "microcrystallite." The rest of the crystal (taken as infinite) was replaced by an elastic continuum. The motion of the atoms in the region of the microscopic treatment, i.e., in the region of the "microcrystallite," was described by classical equations of motion (see Holmes[20] for the justification of this procedure).

Additional boundary forces, elastic and viscous, are used to model the response reaction of the infinite matrix surrounding the "microcrystallite." The chosen dimensions of the "microcrystallite" and its shape were determined by the assigned energy of the primary knock-on atom, the working memory of the computer, and the content of the problem to be solved. Calculation of the cascade of collisions begins with assigning to one of the atoms of the microcrystallite an initial velocity, and it continues until the perturbation decays, and structuring of the damaged region ceases. The large number of atoms (500–1000 even in the first studies) and the consequent large number of simultaneous equations of motion make the problem extremely unwieldy and analytically unsolvable. However, using a computer relieves this difficulty.

The fundamental simplicity of Vineyard's model contrasts with the cumbersome methodology of realizing it. While considering that the problems of realizing the model have already been discussed (see[1,12,21]), we shall restrict the discussion only to adducing here a typical block diagram of the algorithm that is used to model a cascade of collisions (see Table 3, which uses the customary terminology). The reader can find the detailed programs for calculating by Vineyard's model in[22,23].

TABLE 3. Block diagram of the algorithm modeling a cascade of collisions.[23]

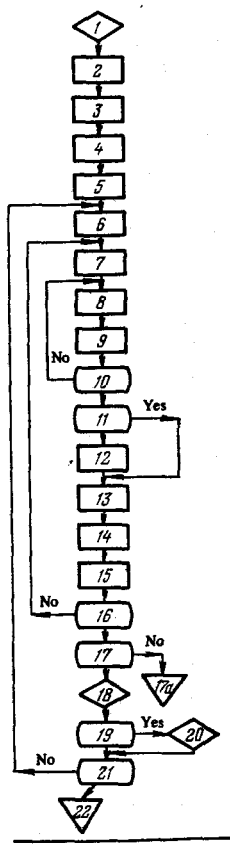

Description of the block diagram

1–Input of information.
2–Construction of the microcrystallite.
3–Marking of surface atoms.
4–Calculation of external forces.
5–Imparting of the initial velocity to the assigned atom into the mass.
6–Start of cycle over the time intervals. Finding of the new coordinates of the entire microcrystallite.
7–Start of the loop over *i*. Choice of the *i*-th atom.
8–Start of the loop over *j*. Choice of the *j*-th atom.
9–Finding the interaction force of the *i*-th with the *j*-th atom.
10–Loop over *j*. Have all the atoms of the microcrystallite been tested?
11–Test of the position of the *i*-th atom. (Is it an internal atom?)
12–Calculation of the elastic and viscous forces of the outer atoms.
13–Calculation of the resultant force on the *i*-th atom.
14–Finding the velocity of the *i*-th atom.
15–Preparation of data for the energy test.
16–Loop over *i*. Has the calculation been made for all the atoms of the microcrystallite?
17–Is the energy test satisfied?
17a–Output for printing of certain information on the energy test. Stop.
18–Output for printing of information on the position of the given atom.
19–Test. Should the coordinates of the entire microcrystallite be output for printing?
20–Output for printing of the coordinates of the atoms of the microcrystallite.
21–Loop over the number of time intervals. (Have all the intervals been counted?)
22–Stop.

A picture could be constructed by using Vineyard's model of the features of the course of the collisional cascades at low energies (the energy E of the primary knock-on atom = 0–1500 eV) and at low temperatures of the irradiated crystal.[1,3,4,24–31] The model made it possible to "see" the cascade of collisions at any instant of its development. As examples, Figs. 2 and 3 give trajectories of colliding atoms in a cascade at dif-

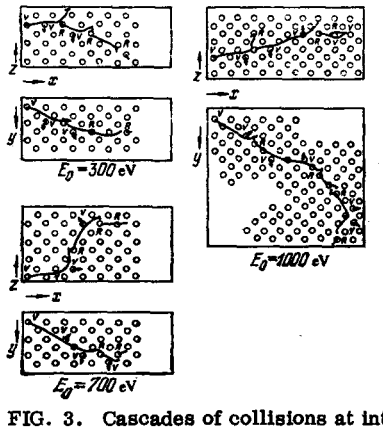

FIG. 3. Cascades of collisions at intermediate energies of the primary knock-on atom in the b.c.c. crystal of α-Fe.[4] The branching is not shown in full, but the trajectories of the most energetic atoms are drawn. *V*—site of vacancy formation, *R*—site of formation of a replacement, E_0—initial energy of the primary knock-on atom.

ferent initial energies of the primary knock-on atom for two types of crystal lattices (f.c.c. and b.c.c.).

They established that the regular arrangement of the atoms on a lattice strongly influences the course of the cascade at low energies of the primary knock-on atom. The entire cascade is divided into a chain of collisions that are especially marked in the close-packed directions. The fundamental mechanism of displacement at low energies is dynamic replacement. The primary knock-on atom itself does not enter an interstice, but replaces one of its neighbors. This can be a nearest, second, or third neighbor, depending on the initial direction of motion of the primary knock-on atom. More remote neighbors can be replaced only at energies above 70 eV (for α-Fe).

The replacements by knock-on atoms form extended sequences of correlated replacements (dynamic crowdions), while interstitials are created at several atomic spacings from the vacancy. As the calculations of cascades imply, these sequences are the most important mechanism that leads to separation of interstitials and vacancies. It was found for a small range of directions that small vacancy clusters can be produced, as well as a single vacancy at the site of the primary knock-on atom.

The stable form of an interstitial in the cited two lattice types has the shape of a dumbbell configuration oriented in the ⟨100⟩ direction for a f.c.c. lattice[1,31] and in the ⟨110⟩ direction in a b.c.c. lattice[3] (see Chap. 4 for fuller treatment of this).

The machine calculations confirmed the hypothesis of the simple cascade theories that a threshold displacement energy (E_d) exists, but they introduced much novelty into its content. First, its definition was changed. The results of modeling show that we should take as the threshold displacement energy E_d^{hkl} the minimum energy needed to form a stable pair of defects in the ⟨hkl⟩ direction, i.e., the energy that we must impart to an atom so that it can form a replacement chain longer than the recombination radius (see Chap. 4).

Second, Vineyard's model showed a strong dependence of the threshold displacement energy on the crystallographic direction. In most cases, stable defects are formed most easily in the ⟨100⟩ direction ($E_d^{100} \cong 22$ eV for copper and $E_d^{100} \approx 17$ eV for α-Fe). The threshold sharply rises near the ⟨111⟩ direction and a number of other directions ($E_d^{111} \approx 80$ eV for copper and $E_d^{111} \approx 55$ eV for α-Fe).

In their experiments, Lomer and Pepper[22] have confirmed the anisotropy of the threshold displacement energy. These authors irradiated a monocrystal of α-Fe of high purity at a temperature below 25 °K with monochromatic electrons of energies 0.3–2.0 MeV, and determined the threshold displacement energies of atoms for the ⟨111⟩ and ⟨100⟩ directions. However, they got the values $E_d^{100} \approx 20$ eV and $E_d^{111} \approx 30$ eV. That is, while they noted the existence of anisotropy near 0 °K, at the same time they showed that this anisotropy is not as sharp as is predicted by Vineyard's machine model. Further studies on machine models, but now with account taken of the thermal vibrations of the lattice atoms, have eliminated this contradiction[37] (see below).

Erginsoy *et al.*[4] have traced the evolution of a cascade of collisions with increased energy of the primary knock-on atom (see Fig. 3). They established by varying the energy of the primary knock-on atom over the range 100–1500 eV that the radiation damage in α-Fe consists in vacancies and interstitials at all energies up to 1500 eV. They did not detect "depleted zones" and defects more complex than small accumulations of vacancies.

As it turned out, the number of Frenkel' pairs increases approximately linearly with increasing energy of the primary knock-on atom according to the formula $N_d \approx E/2E_d$, where $E_d \approx 50$–55 eV. Yet the effect of the crystal lattice is manifested in the appearance of chains of collisions, and it leads to spatial separation of the interstitials and vacancies. The vacancies are mainly concentrated near the primary knock-on atom, and the interstitials on the periphery.

No detailed calculation of the replacements was performed, but their number is about four times as great as N_d. While it has been previously established[3] that the cascade from a primary knock-on atom having an energy below 100 eV resembles a tangle of chains of atom-atom collisions, with increased energy of the primary knock-on atom, this tangle begins to separate into individual tangles (subcascades).

This impression is created by the fact that first the primary knock-on atom and then the secondary displaced atoms possess high energy, and thus they travel for distances of several lattice constants without bringing about replacements, and without stopping in interstices. These motions recall cases of channeling, but they merely resemble them, since no case has been noted in even a single cascade (up to 1500 eV) in which the knock-on atom traveled over a long enough path to be classified as being "channeled."

This observation led the above-cited authors[4] to conclude that channelization processes play no substantial role in the development of radiation damage at low and intermediate energies, except for cases of special irradiation along lattice channels. In their opinion, the fundamental reason is that the probability for atoms that are knocked out from their sites to enter a channel is extremely small.

B. The effect of thermal vibrations on the anisotropy of threshold displacement energies and on propagation of dynamic crowdions

An entire series of studies performed in recent years have repeatedly noted that the temperature of a crystal being irradiated with fast particles substantially affects the dynamics of radiation damage.[20,33–35] In line with these studies, there directly arose the pressing problem that we have studied[37,40] of taking account of thermal lattice vibrations within the framework of the methods of machine modeling of radiation damage in crystals.

Since a cascade of displacements develops at velocities considerably exceeding the speed of sound in the crystal,[36] we can assume that the dynamic damage processes occur as though in a lattice whose atomic thermal vibrations have been instantaneously frozen. The thermal displacements in this case resemble displacements caused by structural defects. Hence the thermal displacements must especially markedly affect those radiation-damage processes for which a regular arrangement of the atoms in the crystal is important, i.e., for example, propagations of chains of atom-atom collisions (focusons, crowdions), channeling, etc. In line with the abovesaid, the question arises of how one should introduce into the equations of motion the thermal displacements of the atoms in modeling radiation damage by Vineyard's method. Owing to atom-atom interaction in the crystal, these displacements are generally correlated.

As Van Hove[38] has shown, the most general correlation relationships in the crystal are reflected by the pair-correlation function in space and time $G(\mathbf{r}, t)$. In the classical case, it describes the mean density of atoms at the point $\mathbf{r}$ at the time t, under the condition that some atom lay at the origin $\mathbf{r}=0$ at the instant of time $t=0$. That is, it describes the correlations in position of two different atoms at different instants of time. The function $G(\mathbf{r}, t)$ is close to the spatial pair-correlation function $g(\mathbf{r})$ if the condition is satisfied that $r_0/v \equiv t_1 \ll t_0$, where r_0 is the radius of action of the correlations, t_0 is the characteristic correlation time, and v is the velocity of propagation of the process. For solids, $r_0 \approx 10^{-8}$ cm, and $t_0 \approx 10^{-13}$ sec. Hence $t_1/t_0 \approx 10^5/v$, with v in cm/sec. Inasmuch as radiation-damage processes propagate at velocities far exceeding the velocity of sound in the crystal, then $t_1 < t_0$, and thus the static approximation is justified.

Along this line, in[37] random (but spatially correlated in the static approximation) thermal displacements of the atoms are introduced as initial conditions into the system of equations of motion of the atoms of the microcrystallite region. After a primary knock-on atom has been generated, these equations are integrated on the computer, and thus an individual realization of the random process is generated. In order to determine the sought quantities (lengths of flight paths, energy losses, etc.), one averages over the results of a large number of realizations, i.e., over all thermal displacements possible at the given crystal temperature. Consequently, it proves possible to take account of thermal displacements while one simultaneously uses the method of statistical trials (the Monte Carlo method) and Vineyard's model.

In[37], the correlation functions of the random displacements of atoms were determined by using the Debye approximation. Table 4 shows the structure of the general modeling algorithm. The block diagram for calculating a single realization is too unwieldy to be given here. Yet in its general features, it resembles the diagram that we have given above (see Table 4). Let us take up in greater detail the physical results obtained here. By using the above-cited modeling algorithm, the problem was solved[40] of the propagation of branches of a cascade of collisions (a chain of correlated atom-atom collisions) in an α-Fe crystal over a broad temperature range.

It was established that a considerable enhancement of energy dissipation arises with the appearance of thermal vibrations in the chains of atom-atom collisions of all types (dynamic crowdions, focusons). With increasing temperature, this leads to a substantial decrease in the flight path of a crowdion. Thus, e.g., the flight path of a crowdion found without accounting for thermal displacements is 22 d in α-Fe in the ⟨111⟩ direction for a primary knock-on atom of energy $E_0 = 50$ eV (d is the interatomic distance). Even when we account for the zero-point vibrations, this flight path declines to 11 d, while at $T = 424$ °K, it shortens further to 8 d.

Since the crowdion mechanism is considered to be one of the reasons for appearance of stable Frenkel' pairs, the problem becomes important of the stability of a vacancy and an interstitial atom lying at such short distances. As Vineyard and his associates showed,[3] a so-called annihilation zone exists around a vacancy (see also Chap. 4). An interstitial atom that falls within it shifts into a normal site, while the vacancy disappears. The dimensions of the annihilation zone were not calculated in accounting for thermal vibrations.

Yet we should expect at the same time that temperature increase would enlarge this zone. If we now take account of the decrease in the flight path of a crowdion with temperature, as we have discussed above, then we conclude that the crowdion mechanism of formation of stable defects generally ceases to operate at high temperatures. At the same time, the importance of this process at low enough temperatures is undoubted.

In line with the problems that we have discussed above, the results of the experiments of Lomer and Pepper[32] that we mentioned in Sec. A of Chap. 3 are of great interest. We recall that, in accord with the results of Vineyard[3] for α-Fe, the threshold displacement energies for different crystallographic directions are: $E_d^{100} = 17$ eV, $E_d^{111} = 55$ eV. At the same time, Lomer and Pepper got the values $E_d^{100} = 20$ eV and $E_d^{111} = 30$ eV. We can understand these experimental data by taking account of the results of the calculations that con-

TABLE 4. Block diagram of the overall algorithm modeling the process of the dynamics of radiation damage with account taken of thermal vibrations.

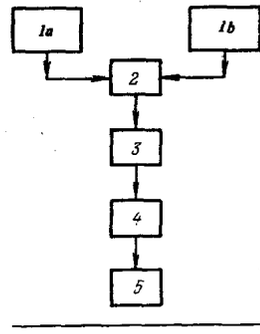

Description of the block diagram

1a–Calculation of the variance of the thermal displacements.

1b–Calculation of the correlation function of the thermal displacements.

2–Solution of the system of equations for finding the coefficients for converting pseudorandom numbers to thermal displacements (Newton's method; see[40] for details).

3–Calculation of the sizes of the thermal displacements.

4–Calculation of a single realization (flight of a chain of atom-atom collisions).

5–Finding of the sought quantities (flight path of a crowdion, etc.).

sidered thermal displacements.

Before we proceed directly to estimating the energy E_d on the basis of such calculations, we note that we must know the dimensions of the spontaneous-annihilation region in order to determine E_d (see Sec. A of Chap. 3). The only existing information on its dimensions currently is that contained in the studies of Vineyard *et al.*[1,3] However, thermal motion was not taken into account there. These studies showed that the annihilation distance in α-Fe is three lattice constants for the ⟨111⟩ direction, and two lattice constants for the ⟨100⟩ direction. Since here the annihilation distances are very small, so that a small number of atoms participates substantially in the annihilation process, we should hardly expect an appreciable effect of thermal motion on the annihilation distance. The latter involves the fact that the mean kinetic energy of an atom in the annihilation region is large at low temperatures in comparison with the mean thermal energy.

Hence, if we assume that the annihilation distance at 25 °K (the conditions of Lomer and Pepper's experiment) has the same value as was found in[1,3], then with account taken of thermal vibrations, we find by using the results of [40] that $E_d^{\langle 111\rangle} \approx 26$ eV, while $E_d^{100} \approx 18$ eV. These values of E_d agree with the experimental data. We note also that the good agreement with experiment of the obtained E_d values indicates also that the size of the annihilation region found in[3] for α-Fe at low temperatures is correct.

The noted substantial decrease in the flight path of crowdions with increasing temperature should lead under these conditions to another effect, namely, spatial localization of the cascade of collisions. This situation hinders efflux of energy from the cascade region, and it should favor the formation of peaks that are analogous in a certain sense to those previously discussed by Seitz, Brinkman, and Koehler.

C. Cascades of collisions at high energies

As Erginsoy *et al.*[4] have shown, cascades that are initiated by primary knock-on atoms of energies below 1.5 keV can be simulated by using Vineyard's model. However, a large fraction of the damage, e.g., in reactor technology, is caused by cascades initiated by primary knock-on atoms having energies in the range 1–1000 keV. If here we follow the path proposed by Vineyard (as is possible in principle), we shall face difficulties involving the limited memory of the computer. Even when simulating a cascade from a primary knock-on atom of energy 1 keV, we must solve about 1500 equations of motion. However, for a cascade, e.g., from a primary knock-on atom of energy 20 keV, we must solve more than 30,000 equations of motion, etc. All of this forces us to take the course of seeking a simpler, but of course cruder approach. One of these approaches to solving the discussed problem is the machine model of dynamic radiation-damage processes that has been intensively developed and used by Beeler and Besco.[2,41–46]

In contrast to Vineyard's method, in which one solves the equations of motion of a large ensemble of bound atoms, the cited authors model high-energy cascades of collisions by tracing the branching sequence of binary collisions of each of the displaced atoms until it finally stops.[3)] One assumes that the participants in the collision in each case are the moving knock-on atom (at the onset of development of the cascade, this is the primary knock-on atom) and a target atom that is at rest at its normal site in the crystal lattice. The directions of emergence of the colliding partners and the energy imparted to the target atom are calculated exactly in the binary-elastic-collision approximation (all this is done within the framework of classical collision theory[48]). The potentials of Erginsoy, Vineyard, and Englert[3] for α-Fe and of Gibson, Goland, Milgram, and Vineyard[1] for Cu were used to describe the collisions in the metals. The potential used in the calculations on tungsten was constructed by combining the Thomas-Fermi potential with the potential of Johnson[49] (See Fig. 1).

In the method of Beeler and Besco, the machine traces the trajectory of the primary knock-on atom until it fully stops, and records here the coordinates, energies and directions of the velocity of all the atoms that were displaced during the motion of the primary knock-on atom. Then the computer analogously traces the trajectories of the secondary displaced atoms, the tertiary, etc. Here one traces first the trajectories of the fastest atoms. An atom is considered to be displaced from its site if the energy imparted to it is above the threshold.[43] In the computer memory, the sites of origin of the displaced atoms are recorded as vacancies, and the stopping sites of the knock-on atoms as interstitials. When the energy of a displaced atom falls below the threshold, the atom is artificially stopped in one of the atomic sites closest to the given point of its motion, which is chosen as the center of a dumbbell interstitial configuration. This configuration is created from the atom that has arrived and the atom that had previously occupied this site. Since all the data on defect formation are recorded systematically in a damage table, this makes it possible to trace also intracascade radiation annealing.

If vacancies exist near a dumbbell that are capable of spontaneous annihilation, then the nearest of them is chosen as the partner for recombination. If there is no such partner, then the damage is taken to be stable, and it is entered in the damage table. Thus, in the theory of Beeler and Besco, the model of the cascade of collisions permits one to use such results of modeling low-energy cascades as the threshold displacement energies, the size of spontaneous-annihilation zones, configurations of interstitials, vacancies, and of clusters of them (see Secs. A and B of Chap. 3).

Let us discuss the fundamental results obtained with the Beeler–Besco model for cubic metals. The form of the trajectories of the cascades of collisions calculated by the model of branching binary collisions is given in Fig. 4, which shows a plane projection of the

[3)] This approximation for computer modeling was first used by Yoshida[47] in studying cascades in amorphous Ge.

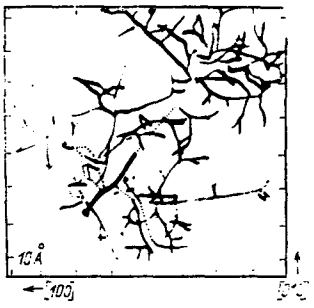

FIG. 4. Projection on the (001) plane of the trajectories of the atoms ejected from their sites in a cascade of collisions in α-Fe.[2] This cascade was initiated by a primary knock-on atom of energy 5 keV that left its site at the lower end of the heavy solid line. The dots are the tracks of the secondary knock-on atoms. The solid thin lines show the trajectories of the knock-on atoms of higher orders.

network of trajectories in the three-dimensional lattice.

As Fig. 4 shows, the size of the region encompassed by the cascade is usually determined by the trajectories of the knock-on atoms of higher orders, rather than the primary and secondary knock-on atoms. In most cases, the energy of the primary knock-on atom (in the range $0.5 \leq E \leq 25$ keV) is fully transmitted to secondary atoms within the range of 10–80 Å of its travel in α-Fe and Cu. The lower limit agrees with the results obtained in Vineyard's model.[4] The spatial distribution of the atoms that collide in the process of development of a cascade is of interest (this includes all the atoms that receive energy). The post-cascade defect distribution is a direct consequence of this distribution. Figure 5 gives an example of the distribution of colliding atoms. It depicts a cross-section of the volume in which the colliding atoms for a 5-keV cascade are concentrated.

Figure 6 shows as an example a post-cascade defect distribution: vacancies, interstitials, and clusters of them, which is here the most important result. Tables 5–9 give the data on them. They are averages that are obtained over a large number (about 10^2) cascades having the same initial energies, but with different initial directions of motion of the primary knock-on atom, which is chosen randomly each time by starting with a uniform angular distribution.

It was found in modeling cascades in the region of high initial energies of the primary knock-on atom (0.5–20 keV) that the largest of the "embryonic" clusters found in α-Fe and Cu were clusters of vacancy type, and they contained about 20 vacancies. At the same time, the clusters of interstitial atoms were much smaller: the largest in α-Fe and W were triple interstitials, and in Cu quadruple interstitials. Perhaps this stemmed from

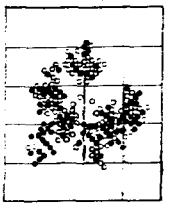

FIG. 5. Projection on the (001) plane of the colliding atoms in a layer two lattice constants thick.[2] The cross-section is taken through the volume of a cascade of collisions from a primary knock-on atom of energy 5 keV (●, □—atoms of the upper and lower layers).

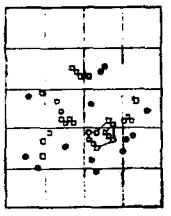

FIG. 6. Distribution of vacancies (□) and interstitials (●) resulting from a cascade from a primary knock-on atom of energy 5 keV.[2]

the fact that the spatial defect distribution in the studied metals had the shape of a nucleus enriched in vacancies and an envelope in which individual interstitials lay. This pattern fits the ideas of Brinkman on the structure of a displacement peak and of Seeger on the "depleted zone."

We can clearly see from Tables 6 and 7 the changes that occur in the size distribution of the vacancy clusters as a function of the initial energy of the primary knock-on atom. The relative total number of clusters $V(1) + V(2) + V(3)$ as averaged over all the cascades having a given energy remains approximately constant. This configuration contains 68% of the vacancies formed in α-Fe, and about 73% in Cu.

The low-energy (0.5–2.5 keV) size distribution of "embryonic" clusters that contain more than three vacancies differs from the high-energy distribution (5–20 keV) (see Table 7). In α-Fe, large clusters (≥ 10 vacancies) exist only in the high-energy distribution, and mean number of them increases with increasing energy of the primary knock-on atom. This leads to a great variety in the cluster configurations for large energies of the primary knock-on atom. As we have stated, in the energy range of the primary knock-on atom from 0.5 to 20 keV, the interstitial atoms produce almost exclusively only single, double, or triple inclusions. At least 99% of the interstitials that arise in copper fall into these configurations. In α-Fe, 99.5% of the interstitials are found in these configurations.

Table 9 gives the size distributions of the "embryonic" clusters of interstitials as a function of the initial energy of the primary knock-on atom. As Beeler[50] points out upon comparing the conclusions of the machine experiment with the experimental studies of the damaged state by the ion-microscopic method, there is good qualitative agreement for f.c.c. and b.c.c. systems.[51,52] There is agreement for the volume of the damaged region for a given energy of the primary knock-on atom, for the size distribution of vacancy clusters, and for the rearrangement of vacancies in the damaged region.

In concluding, we stress again that the model de-

TABLE 5. The volumes encompassed by the cascade of atomic collisions in α-Fe and copper (in units of the atomic volume).

Energy of the primary knock-on atom, keV	Volume encompassed by the cascade of collisions		Energy of the primary knock-on atom, keV	Volume encompassed by the cascade of collisions	
	α-Fe	Copper (Cu)		α-Fe	Copper (Cu)
0.5	300	450	10	4550	6300
1	550	800	15	7150	9250
2.5	1320	1750	20	9500	12250
5	2350	3350			

TABLE 6. Fraction of the total number of vacancies contained in an n-vacancy cluster for the post-cascade defect distribution in α-Fe.

Size of the cluster (n-vacancies)	Energy of the primary knock-on atom, keV						
	0.5	1	2.5	5	10	15	20
1	0.352	0.326	0.328	0.336	0.350	0.356	0.351
2	0.208	0.194	0.211	0.191	0.202	0.193	0.203
3	0.129	0.125	0.125	0.145	0.135	0.129	0.131
4—6	0.254	0.243	0.196	0.244	0.202	0.196	0.203
7—9	0.057	0.112	0.090	0.057	0.072	0.079	0.070
$\geqslant 10$	0	0	0.04	0.057	0.039	0.047	0.042

scribed above and Vineyard's model are currently the fundamental machine models for studying radiation defects. Their special signficance consists in the fact that they permit one to study not only elementary processes of radiation damage (focusons, crowdions, annihilation zones, etc.) but also to find the size distributions of clusters of different types. Under irradiation conditions of this type, "embryonic" clusters can exert a substantial influence on the course of various physical processes. In particular, in materials undergoing fission, it is precisely their number and size distribution that determines the mechanism of production of gas pores (see[52] for the kinetics of gas expansion in the homogeneous and heterogeneous creation of gas pores).

D. Cascades of collisions in diatomic crystals

Wigner has also discussed the disordering action of irradiation.[53] It has also been observed repeatedly in the series of ordered alloys (e.g., Cu_3Au and Ni_3Mn[54]). One of the possible processes explaining this disordering is the propagation of chains of substitutional collisions. This hypothesis has stimulated machine calculations of dynamic processes of radiation damage in binary crystals. Vineyard[25] has undertaken modeling of the dynamics of radiation damage in binary crystals for Cu_3Au, Torrens, Chadderton, and Morgan[55,56] for the alkali halides, and Jackson, Leighly and Edwards[57] for Fe_3Al. All of these authors used the Brookhaven method in their calculations.[1]

As we have noted above, difficulties arise directly in the choice of the interaction potential for binary crystals when one uses this method. While not reporting the data on the potentials that he had used for ordered Cu_3Au, Vineyard[25] first noted the interesting feature of propagation of chains of atom-atom collisions along the ⟨100⟩ direction in this alloy. The heavy gold atoms and light copper atoms alternate in the ⟨100⟩

TABLE 7. Fraction of the total number of vacancies contained in an n-vacancy cluster for the post-cascade defect distribution in copper.

Size of the cluster (n-vacancies)	Energy of the primary knock-on atom, keV						
	0.5	1	2.5	5	10	15	20
1	0.377	0.362	0.350	0.372	0.378	0.384	0.392
2	0.200	0.225	0.222	0.213	0.200	0.214	0.218
3	0.160	0.129	0.129	0.136	0.135	0.139	0.131
4—6	0.213	0.200	0.205	0.180	0.203	0.185	0.180
7—9	0.030	0.070	0.059	0.068	0.053	0.048	0.052
$\geqslant 10$	0.020	0.014	0.035	0.031	0.031	0.030	0.027

TABLE 8. The fraction and mean number of vacancies in an n-vacancy cluster for low- and high-energy cascades in copper and α-iron.

Metal and energy of the primary knock-on atom, keV	Size of cluster (n-vacancies)					
	1	2	3	4—6	7—9	$\geqslant 10$
Cu: 0.5—1	0.37	0.21	0.14	0.21	0.05	0.02
2.5—20	0.38	0.21	0.14	0.19	0.06	0.03
$\bar{n}$	1	2	3	4.6	7.7	12.3
Fe: 0.5—1	0.34	0.20	0.13	0.23	0.10	—
2.5—20	0.35	0.20	0.13	0.21	0.07	0.04
$\bar{n}$	1	2	3	4.7	7.7	12.2

direction. After a collision of a light copper atom with a gold atom, the former performs a to-and-fro motion between the two nearest Au atoms. These multiple impacts nevertheless permit the oscillating Cu atom to transfer most of its kinetic energy to an Au atom, and in spite of the original expectations, the chain of collisions reliably propagates along ⟨100⟩ at energies of the primary knock-on atom from 25 to 100 eV, thus leading to appreciable disordering.

Torrens, Chadderton, and Morgan[55,56] have made more detailed calculations for diatomic crystals. They studied the motion of the ions in crystals of potassium and sodium chlorides. In potassium chloride, the alkali and halide ions are about equal in mass, while in sodium chloride, their masses are approximately in the ratio 2:1. The "microcrystallite" of the model contained 1000 ions. Two components were taken into account in modeling the interaction of the ions: the electrostatic force (attractive or repulsive, depending on the signs of the interacting ions), and a repulsive force that stems from the overlap of the closed electron shells of adjacent ions. The electrostatic component was described by the potential

$$V(r)_{\text{electrostat}} = \frac{\alpha e_1 e_2}{\varepsilon r}, \qquad (5)$$

Here α is the correction for polarization of the ions (it was approximately 0.5 for KCl and 0.64 for NaCl, e_1 and e_2 are the charges on the ions, ε is the d.c. dielectric constant (which was taken to be 1 for nearest neighbors, and 2 for all the subsequent ones).

The second component was described by the potential

TABLE 9. Fraction of the total number of interstitials in an n-interstitial cluster for the post-cascade defect distribution in α-Fe and Cu.

n	Energy of the primary knock-on atom (keV)						
	0.5	1	2.5	5	10	15	20
				α-Fe			
1	0.98	0.97	0.96	0.95	0.94	0.94	0.94
2	0.02	0.03	0.04	0.05	0.06	0.06	0.06
3	0	0	0.002	0.001	0.003	0.003	0.003
				Cu			
1	0.97	0.95	0.93	0.92	0.90	0.90	0.91
2	0.03	0.05	0.07	0.07	0.09	0.09	0.08
3	0	0.003	0	0.01	0.01	0.01	0.01
4	0	0	0	0	<0.001	<0.001	<0.001

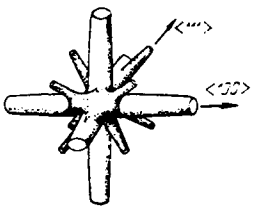

FIG. 7. Relationship of the threshold displacement energy to the direction of motion of the ion in KCl. [58]

$$V(r)_{\text{repulsive}} = \frac{\Lambda}{r^n}, \qquad (6)$$

Here $n = 9$ for K^+–K^+, K^+–Cl^-, and Cl^-–Cl^- interactions, $n = 8$ for Na^+–Cl^- interactions, and $n = 7$ for Na^+–Na^+ interactions. The quantity Λ for each of the potentials was found by fitting the equilibrium ion configuration in the model crystal to the actual configuration.

As the modeling calculations showed, the threshold displacement energy for the two salts is anisotropic, and it has a minimum near the ⟨100⟩ direction. This threshold is about 25–30 eV for KCl (K and Cl), and it varies over the range from 20 eV (Na) to 90 eV (Cl) for NaCl. In the latter case, the large mass difference of the Na and Cl ions exerts an effect. The threshold has a maximum above 150 eV in the ⟨100⟩ and ⟨111⟩ directions (Fig. 7). Separation of a vacancy-interstitial atom pair occurs by chains of replacements. The alkali and halide ions in both salts formed interstitials as a configuration of a static crowdion along ⟨110⟩ (Fig. 8).

While taking account of the fact that the displacement process in ionic crystals is of interest from the standpoint of production of color centers, Chadderton, Morgan, and Torrens tested several possible mechanisms of their production. In particular, they studied with a computer the feasibility of the mechanism proposed by Varley.[58] According to Varley, a multiply ionized halogen ion must leave its place in the prior arrangement owing to strong repulsion from the six alkali ions that surround it. Within the framework of their model, Chadderton, Morgan, and Torrens[55,56] got a result that contradicts Varley's mechanism. The motion of the multiply ionized ion took place along the ⟨110⟩ and ⟨111⟩ directions, but the expected replacements were not observed.

The last of the models of the dynamics of radiation damage in binary alloys known to us was that of Jackson, Leighly, and Edwards[57] for the ordered crystal Fe_3Al (Fig. 9). The "microcrystallite" contained 559 atoms bound by pairwise interaction forces (Fe–Al and Fe–Fe). These authors neglected the Al–Al interaction, owing

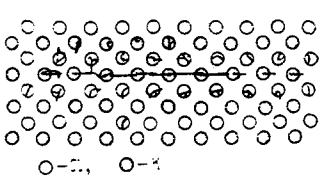

FIG. 8. Conversion of a dynamic into a static crowdion. 30 eV energy was imparted to a K ion at an angle of 5° to ⟨110⟩. This produced a symmetrical interstitial in the form of a crowdion on the line ⟨110⟩ at a distance of six lattice constants from the primary knock-on atom.

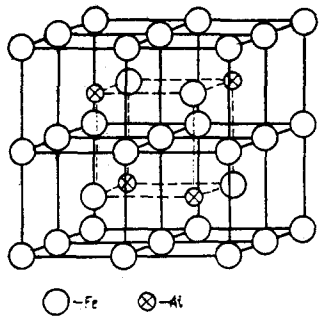

FIG. 9. Unit cell of the superlattice of Fe_3Al.

to the large distance between these atoms.

They calculated cascades of collisions with different energies and initial directions of velocity of the primary knock-on atom, without taking account of thermal vibrations. Just as in monatomic crystals, the threshold energy needed to produce a stable atomic displacement in Fe_3Al proved to depend strongly on the direction of motion of the primary knock-on atom. Thus the threshold energy in a ⟨100⟩ chain consisting of iron atoms proved to be 22 eV (cf. the value 17 eV in pure α-Fe found by Erginsoy *et al.*[3]).

Yet in the ⟨110⟩ direction, the threshold proved to be 44 eV. Interestingly, in both α-Fe and Fe_3Al, the threshold in the ⟨110⟩ direction proved to be two times as great as that in the ⟨100⟩ direction. The ⟨111⟩ direction in the Fe_3Al crystal appreciably differs from the ⟨110⟩ and ⟨100⟩ directions, where the chains of atoms contain only iron atoms or only aluminum atoms. Namely, the ⟨111⟩ chains in Fe_3Al contain aluminum atoms separated by three iron atoms (Fig. 10), so that they must possess several (four) threshold displacement energies.

It turned out that a stable displacement does not occur (up to the energy 98 eV), independently of the original site of the primary knock-on atom. The longest chains of collisions develop when the primary knock-on atom is an iron atom. In all cases, the presence of the Al atoms in the chain hindered energy transfer along it. As compared with pure iron, a large initial kinetic energy was required to initiate replacement chains having the same length in Fe_3Al. Whenever the primary knock-on atoms were directed at small angles to the axis of a chain, the presence of the Al atoms always caused an additional defocusing (Fig. 11).

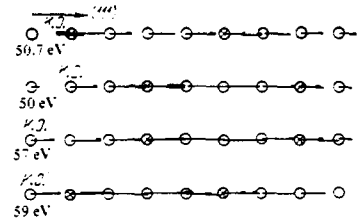

FIG. 10. Chains of collisions in the ⟨111⟩ direction (Fe_3Al). The energies of the primary knock-on atoms (K. O. = knock-on) initiating the chains are indicated at the left.

Moreover, an additional defocusing was also noted in the case in which the aluminum atom occurred in "lenses" (in the immediate environment of the chain) (Fig. 12). This arose from the small mass of the Al atoms as compared with the Fe atoms (the light atoms of Al have a greater tendency to be displaced from their normal lattice sites than the Fe atoms). Whenever the chain of collisions was surrounded alternately by Al and Fe atoms, and was originally initiated in the ⟨100⟩ direction, it showed a tendency to rotate into the (100) plane where rows of Al atoms lie.

Most of the chains of collisions follow the ⟨100⟩ and ⟨110⟩ directions, which, as we have pointed out, consist completely of Al or Fe atoms. Hence the disordering in these directions proved to be small. It was previously assumed that the greatest disordering must occur in propagation of chains of collisions in the ⟨111⟩ direction, which consists of Al and Fe atoms. However, a replacement chain arises in this direction with difficulty, and hence also here the disordering proved to be small (at energies up to 89 eV).

In concluding, we should note that one observes general regularities in all cases, although the above-cited results were obtained for three different types of binary crystals (Cu_3Au, alkali halides, and Fe_3Al). Just as in the monatomic materials, the final static damage consists of Frenkel' defects that are produced by the passage of chains of replacements (dynamic crowdions). In none of the studied cases do the primary knock-on atoms themselves become interstitials. However, the interstitials are produced in the form of a dumbbell configuration or a static crowdion.

The threshold displacement energy shows a clearly expressed anisotropy, but it is larger in magnitude than in monatomic crystals, owing to the inhomogeneity of atomic composition of the chains of collisions. This same inhomogeneity is responsible for the additional defocusing and the additional anisotropy in the propagation of the chains: the chains in the directions having a homogeneous atomic composition have greater flight paths than those in directions of inhomogeneous composition.

The results indicate that dynamic disordering is created only by high-energy chains of collisions with defocusing. However, stable replacements are generally lacking at low energies in the directions where the types of atoms alternate. Experimentally, this effect

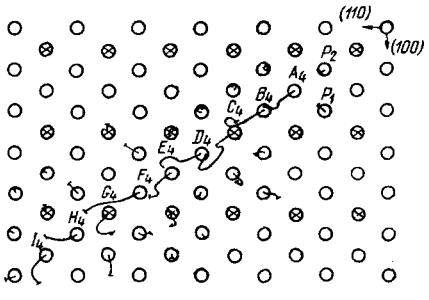

FIG. 11. A chain of collisions in the ⟨111⟩ direction with an initial energy $E_0 = 107$ eV and an initial angle to the axis of the chain $\theta_0 = 1°$ (Fe_3Al).

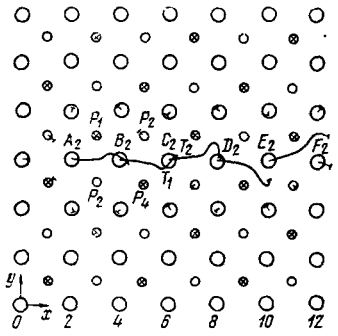

FIG. 12. Defocusing in the ⟨100⟩ direction at an initial energy $E_0 = 107$ eV (Fe_3Al).

must lead to absence of a disordering process at low enough energies of the bombarding particles. In fact, the conclusions that we have drawn above hold only when the thermal motion of the atoms is neglected. As has been shown for the monatomic metals (see Sec. B of Chap. 3), the role of thermal vibrations can prove to be decisive, so that we must make the appropriate generalization of the models treated in this section.

4. MODELING OF DEFECTS THAT ARISE DURING IRRADIATION, AND THEIR INTERACTIONS

Currently, discrete computer models are used widely for modeling atomic defect configurations, the displacement fields around them, and interactions of defects, as well as for determining others of their most important characteristics.

Modern experimental technique permits us to observe directly crystal-lattice defects and accumulations of them (clusters) that arise from irradiation. Clusters of dimensions above 5–10 Å can be observed directly by transmission electron microscopy (see[59–62]). The major defect of this method involves the impossibility of observing lattice defects of diameter below 5 Å. One cannot determine the type of defects if their dimensions are too small even if their concentration is high.

Part of these difficulties is eliminated when one uses a field ion microscope, which permits one to observe small clusters, individual vacancies, and interstitial atoms,[63–66] though indeed only for materials having high melting points. Nevertheless, application of these two methods together with the theory of image contrast in transmission electron and field ion microscopes has made it possible to make certain advances in studying the defect structure of irradiated specimens.

The defects in an irradiated specimen have been shown to have a complicated size distribution (Fig. 13) that depends strongly on the irradiation conditions (temperature, dose, type of radiation, and energy spectrum of the radiation).[67,69–71] The defects change in shape while changing in size. In micrographs, they are ring-shaped in the large size range. Smaller defects (below 50 Å) can be seen in the form of triangles, squares, or "black dots."

In order to understand what the experimenter actually sees when he studies defect structures, we must know how to identify the observed structures with con-

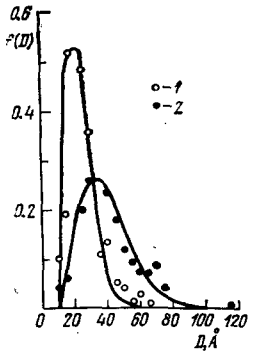

FIG. 13. The experimental size distributions of vacancy clusters[67] for cases of irradiation by protons of energy 0.7 MeV (1) and by fast neutrons (2) are described satisfactorily (solid lines) by the Rayleigh distribution; $f(D)=A(D/\Delta^2)\times\exp(-D^2/2\Delta^2)$ (D is the diameter of the cluster, and A and Δ are constants).[68]

crete atomic configurations. The hope of getting information on these configurations and on the evolution of the configurations as the number of simple defects entering the cluster increases is now directly tied to the potentialities of discrete machine models.

Moreover, we should naturally expect from the machine models information also on the interaction of defects with one another. Yet a knowledge of the possible reactions involving defects might cast light also on the rearrangement of the defect distribution in the processes of irradiation and annealing. The above-mentioned hopes have proved to be to a certain extent justified.

TABLE 10. Block diagram for calculating the atomic configuration of vacancies, interstitials, and complexes of them.[80]

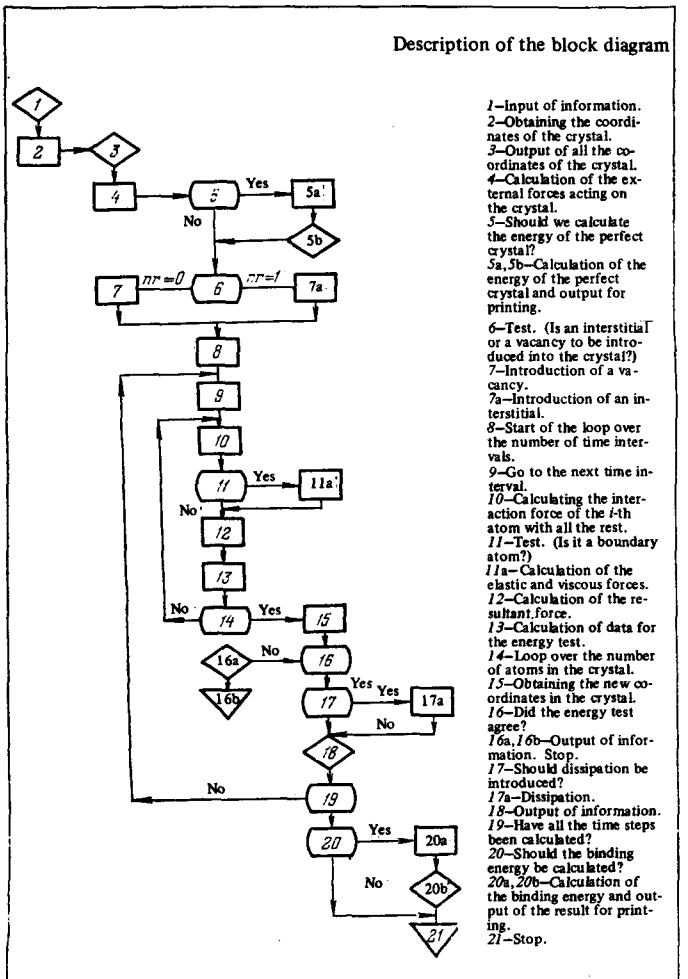

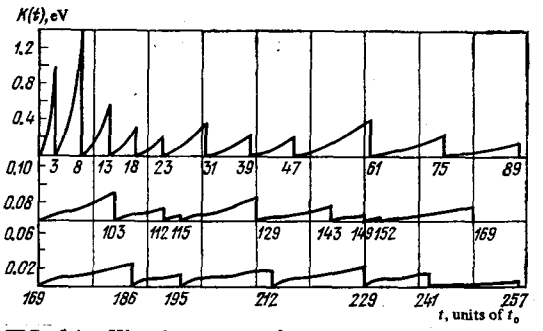

FIG. 14. Kinetic energy of a system with artificial dissipation as a function of the time ($t_0\approx 2.4\times10^{-15}$ sec) in the problem of a complex of two interstitials.[28]

A. Modeling of atomic configurations and determination of the fundamental chracteristics of radiation defects

Two fundamental approaches have been laid out in modeling atomic configurations of defects: the use of discrete models that recall in essence the model of Vineyard that we have already discussed for dynamic cases of radiation damage,[1] and the use of models analogous to that of Johnson.[5–7,49,72–74] [4)]

In the former case, one adopts in the initial conditions a test configuration of a defect, while the atoms of the microcrystallite are assumed to be at rest, or if the test configuration is symmetrical, one imparts to some atom a small initial energy that gives rise to further rearrangement. The computer then solves the equations of motion of the atoms until a static defect configuration is actually reached. Thus, studies were made of configurations of vacancies, interstitial atoms and complexes of them, of the stability of Frenkel' pairs, etc.

For the sake of economizing computer time and for faster establishment of an equilibrium defect configuration in the microcrystallite, Gibson, Goland, Milgram, and Vineyard[1] have proposed introducing an artificial energy dissipation. When the overall kinetic energy of the system reaches a maximum, the velocities of all the atoms in the same configuration are artificially equated to zero, and thus this operation is carried out periodically.[5)]

Inasmuch as it is sometimes hard to establish the exact value of this maximum (owing to appearance of false bursts on the time-decay curve of the energy), one can also apply artificial dissipation in a somewhat different form.[28,79] Namely, the kinetic energy of all the atoms is artificially made zero at a previously fixed instant of time (Fig. 14).

After the kinetic energy of the system has decreased by about three orders of magnitude, the artificial decay is removed, and the configuration is tested for stability by an extra calculation. Table 10 gives a block diagram of a typical calculation of the atomic defect configuration by Vineyard's model.

[4)] Huntington and Seitz,[75] Eshelby,[76] Tewordt,[77] Seeger and Mann,[78] and Johnson and Brown[72] have participated in creating this model. Johnson has been using it most actively.

[5)] Artificial dissipation of energy does not affect the form of the sought stable defect configuration, but it decreases the characteristic time of relaxation of the system toward it.

TABLE 11. Characteristics of the defects found from the modeling calculations.

Metal	Defect											
	Vacancy			Divacancy		Trivacancy		Tetravacancy	Single interstitial			Di-interstitial
	E_m	E_f	ΔV	E_m	ΔV	E_m	ΔV	ΔV	E_m	E_f	ΔV	E_m
Cu	0.42[72,73]	0.40 72.73 0.89	0.53[81] 0.48[72]	0.07[73]	1.0[81]	0.66[82]	1.5[81]	1.5–2.0[81]	0.05[72]	2.20[72]		0.26[72]
α-Fe	0.68[82] 0.68[6]		0.66[82] 0.66[6] 0.78[6]		0.16				0.33[6]			0.18[6]
γ-Fe	1.32[5]	1.49[5]							0.15[5]	4.08[5]		
Ni	1.32[5] experiment 1.5[83]	1.49 experiment 1.48[83] 1.35[84]										

E_m is the activation energy for displacement of defects (eV), E_f is the energy of formation of a defect (eV), ΔV is the change in volume of the crystal per defect (in units of the atomic volume).

The currently very popular model of Johnson differs from that of Vineyard mainly in the methodology of numerical calculation of the stable atomic defect configurations. Just as in Vineyard's model, the atoms of a restricted region of the lattice of the "crystallite" are treated as particles that interact with one another. A central pairwise interaction ϕ_{ij} (see Table 1) between the atoms is adopted, and it is taken into account for neighbors in the two nearest coordination spheres.

In Johnson's model, the crystallite is surrounded by an elastic medium which the rest of the lattice atoms are arranged. In contrast to Vineyard dynamic model Johnson's model can be called static, since the motion of the atoms is not considered in it, while one seeks by an iteration method only the minimum potential energy of the system.

By using the cited computer models or their analogs, various authors have calculated a number of very simple defects and accumulations of them whose existence might be expected in irradiated materials. They have determined in the calculations the following characteristics of the defects: the atomic configuration, the binding energy of the clusters, the activation energy for displacement, the dimensions of the defects, the volume changes per defect, etc. The existing results of these calculations are extensive. They are given for a number of very simple defects in Table 11. Figure 15 gives the atomic configurations of some very simple defects in b.c.c. crystals. The defect structures are arranged

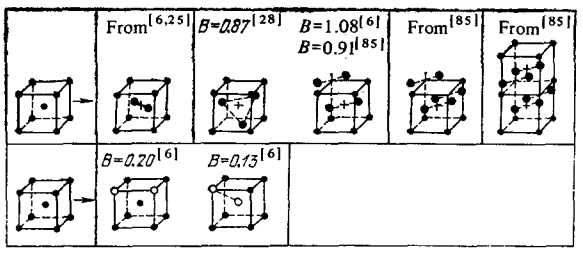

FIG. 15. Atomic configurations of very simple defects in b.c.c. crystals. B is the binding energy of the defects in the cluster (eV), ● —atoms participating in formation of an interstitial defect, ○—vacancies. The displacements of the atoms of the environment are not shown.

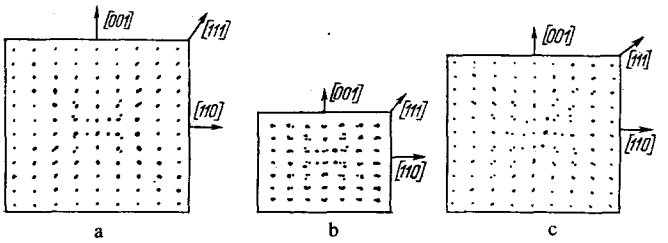

FIG. 16. Evolution of the configuration of an interstitial atom in α-Fe.[85] a) Projection on the (110) plane of the atoms displaced about a bi-interstitial; b) projection on the (110) plane of the atoms displaced about a tri-interstitial; c) projection on the (110) plane of the atoms displaced about a cluster of four interstitials.

in order of increasing number of the elementary defects entering into them. We should immediately note that one cannot consider this to be an exclusive characteristic of a cluster, since even clusters that have the same number of elementary defects can differ in atomic configuration. For example, as model calculations have shown,[25] in a f.c.c. lattice, a cluster of two interstitial atoms has at least three stable atomic configurations.

The atomic configuration of a cluster is its most important characteristic. It includes also the description of the atoms lying in the immediate vicinity of the defect. The displacements of these atoms from their sites are in most cases anisotropic.

The evolution of cluster configurations with increasing size is of especial interest. Bullough and Perrin[85] have studied this problem most systematically. By using a model of α-Fe constructed by analogy with Vineyard's model and consisting of blocks from 2000 to 5488 interacting atoms, they traced the evolution of the atomic configuration of a cluster made of interstitials. Figure 15 shows the initial stage of this evolution.

They adopted a dumbbell configuration (split interstitial) in the ⟨110⟩ direction for a single interstitial, which agreed with Vineyard's results.[25] A bi-interstitial consisted of a pair of split interstitials having axes parallel to one another and parallel to the ⟨110⟩ direction. The binding energy of a bi-interstitial proved to be 0.91 eV, which is lower than that given by Johnson[6] (1.08 eV). Figure 16a shows the pattern of relaxation of the atoms around a bi-interstitial as a projection of the atomic configuration on the (110) plane. Just as for a single interstitial, they observed preferential relaxation of the atoms along the ⟨111⟩ direction.

For a cluster consisting of three interstitials, they found that the only stable configuration for it is one in which three parallel split ⟨110⟩ interstitials form a plate in the {110} plane. This is an important result, since it leads to a two-dimensional shape of the nucleus, and it determines its plane of nucleation. Figure 16b shows the arrangement of interstitials and the relaxation of the atoms in the vicinity.

The choice of the plane of nucleation is consolidated when the next interstitials are added (see Figs. 16c–19). They prolong the plate in the {110} plane, but here one

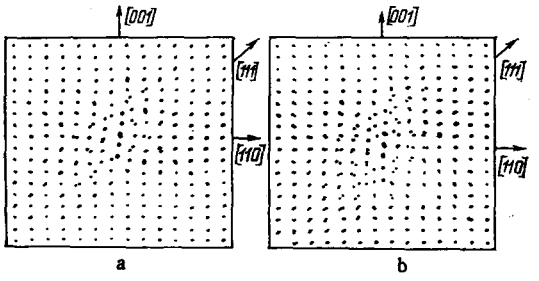

FIG. 17. Evolution of the atomic configuration of an interstitial cluster in α-Fe.[85] Projection on the (110) plane of the atoms displaced about clusters consisting of nine (a) and 16 (b) interstitial atoms. In the latter case, the boundary atoms are fixed in place.[85]

notes a tendency to removal of the stacking fault by shear in the [001] direction.

As the plate grows, the stacking fault is gradually removed, until it vanishes completely for 16 interstitials, and the plate becomes a complete dislocation loop with the Burgers vector $a/2$ [111] (see Figs. 18, 19). Such interstitial loops have actually been observed after low-temperature irradiation.[86,87]

The evolution of a vacancy-type cluster has not been studied as thoroughly as Bullough and Perrin have done for an interstitial-type cluster. Vineyard modeled a set of clusters up to a pentavacancy,[81] and found that combination of vacancies is energetically favorable. That is, vacancy clusters have a positive binding energy. Moreover, he established that the number of stable configurations increases as the vacancy cluster grows.

Analysis of the atomic configurations of pentavacancies indicates that two pathways of further growth of vacancy clusters are possible: either in the form of disks of atomic thickness, or in the form of bulk structures that subsequently serve as the nuclei of pores. The first pathway of development has been studied by A. N. Orlov and R. D. Dokhner, and by Yu. M. Plishkin and I. E. Podchinenov.

Orlov and Dokhner[88] used a model that fundamentally recalled that of Johnson, and treated a cluster of seven vacancies in the (111) plane of a f.c.c. crystal. They calculated the initial positions of the atoms surrounding

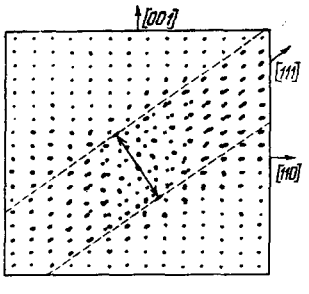

FIG. 18. A cluster of 16 interstitials in α-Fe in which the boundary fixation is released and the boundary atoms are elastically displaced.[85] The plate of interstitials becomes a dislocation loop, which reduces its gliding energy in {111} by rotating in $B'D'$.

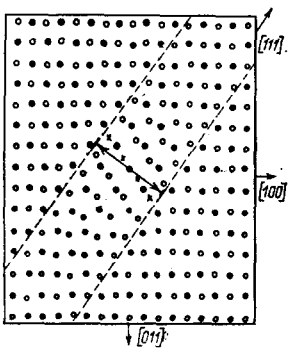

FIG. 19. A section of the atomic configuration of a cluster of 16 interstitials in α-Fe (along the (011) surface of the glide prism[85]). The final position of the side of the loop. ●—atoms of the upper plane; ○—atoms of the lower plane.

the vacancy cluster within the framework of elasticity theory.[89] In this calculation, the studied cluster was represented by a polygonal dislocation loop. The atoms far from the nucleus of the defect were fixed in their positions, while the equilibrium coordinates of the atoms of the nucleus of the defect were determined by minimizing the energy of the set of these atoms, whose interaction was described by a Morse potential. The minimization was done on a computer.

The calculations indicated that the layer of atoms directly adjoining the vacancy complex is displaced in such a way perpendicular to its plane u_x that the atomic planes adjacent to the plane of the cluster approach one another strongly. The distance between them (d_1 in Fig. 20a) becomes equal to $1.3d$ (d is the normal interplanar distance). Yet the displacements of the atoms parallel to the plane of the cluster u_r are considerably smaller in size, and they do not vary monotonically with distance near the plate (Fig. 20b).

The energy of formation of a cluster of seven vacancies $E_f^7 = 18.94$ eV, while the binding energy $E_B^7 = 6.22$ eV. Since it has such a significant binding energy, this cluster is a stable defect, and it can subsequently serve as the nucleus of a prismatic dislocation loop.

Such calculations have also been performed for a hexagonal cluster of large radius formed from the given one by removing the next row of atoms. That is, it consisted of 19 vacancies. They led to analogous results, and here $d_1 = 1.1$ (see Fig. 20). This means that the adjacent planes are so close that the structure produced can be treated as a well-defined dislocation loop.

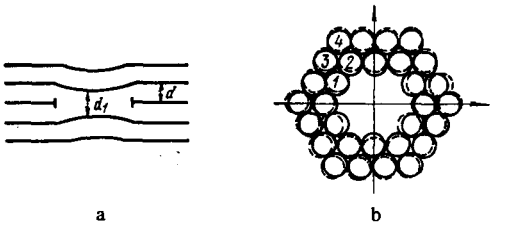

FIG. 20. Displacements of the atoms surrounding a cluster of seven vacancies.[89] a) Deformation of the {111} planes near the cluster (d is the normal interplanar distance, and d_1 is the distance between the planes adjacent to the plane of the vacancy disk); b) the region of the {111} plane that contains the cluster. The dotted lines show the displacements of the atoms. The displacements in units of the interatomic distance are: 1—0.040, 2—0.029, 3—0.014, and 4—0.011.

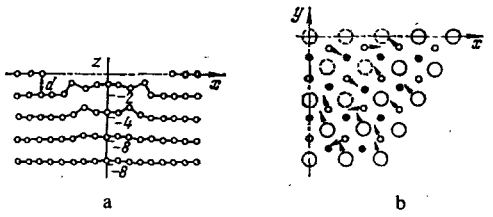

FIG. 21. Displacements of the atoms about a vacancy cluster made of 19 vacancies.[90] a) Projection on a plane perpendicular to the plane of accumulation (the distances are indicated in Å); b) projections of the atoms of the planes lying above (small open circles) and below (solid circles) the plane of the defect (the dotted circles correspond to the vacancies).

The same cluster consisting of 19 vacancies has been calculated by Plishkin and Podchinenov[90] by using Vineyard's model. Calculation of the atomic configuration showed that a prismatic dislocation arises along the boundary of the vacancy plane. In contrast to the solution obtained by Orlov and Dokhner, which gave a single type of direction of displacement of atoms (away from the center in the plane of the defect and toward the center in the adjacent planes), Vineyard's model led to a rather complex geometry of displacements (Fig. 21) that recalls the pattern of displacements of the atoms around a solitary vacancy in which the atoms in the different coordination spheres have different signs of displacement.

B. Interaction of defects

Among the calculations modeling the static interaction of defects with one another, the first were the calculations on the stability of a Frenkel' defect in Cu,[1] and then also in α-Fe.[31] At first the configuration of the interstitial atom (a dumbbell configuration) was calculated with Vineyard's model. Then one of the lattice sites in the vicinity of the interstitial atom was vacated (a vacancy was created), and the subsequent calculations, which were now for a Frenkel' pair, were carried out with the initial conditions thus obtained.

Thus they established (for α-Fe) that all close pairs thus formed are unstable with respect to recombination for any orientation of the line linking the vacancy with the mass center of the dumbbell interstitial configuration. All second neighbors also proved to be unstable with respect to recombination (Fig. 22). Yet if the axis of the defect lay in the close-packed direction ⟨111⟩, the minimum separation of the defects of a stable pair was especially large. The situation in copper was analogous.

Dokhner[91] and Plishkin and Podchinenov[90] have modeled the interaction of point defects with dislocation loops. Dokhner used the modeling method that had previously been used for determining the configuration of a vacancy cluster,[88] and studied the interaction of the nucleus of a prismatic dislocation loop consisting of seven vacancies in the (111) plane of a f.c.c. crystal with a close-lying vacancy.

The calculations determined the interaction energy of the vacancy with a cluster consisting of n vacancies. This energy is equal (with opposite sign) to their binding energy E_B^i (i is the number of the lattice site at which the vacancy occurs):

$$E_B^i = E_f^{1,0} - E_f^{1,i}, \tag{7}$$

That is, it equals the difference between the energies of formation of a solitary vacancy ($E_f^{1,0}$) and a vacancy in the presence of a defect cluster (a dislocation loop) ($E_f^{1,i}$).

The analysis of the performed calculations showed that we can approximate analytically the interaction energy for $0 \leqslant \theta \leqslant \pi$ (θ is the polar angle with respect to the contour of the dislocation):

$$E_B(r, \theta) = Ar^{-n}(1 - B\sin\theta), \tag{8}$$

where r is the value of the radius vector from the vacancy to the dislocation line. For copper, $A = 0.575$ eV, $n \approx 2.2$, and $B = 0.46$ (r is in units of the closest interatomic distance).

One can establish from the $E_B(r, \theta)$ relationship found in[91] that the binding energy of a vacancy cluster with a vacancy lying in an adjacent plane near the center of the cluster is small. Thus it is more favorable energetically for the loop to combine with vacancies in its plane than in planes adjacent to it near its center (which would lead to reorganization of the loop into a volume accumulation of vacancies). Thus, as we should expect, vacancies tend to enter compressed, rather than dilated regions of their environment. Yet a prismatic dislocation itself has a tendency to grow in its own plane, owing to this type of interaction, rather than to reorganize into pores.

Plishkin and Podchinenov[90] used Vineyard's model to treat the interaction of a vacancy with a cluster consisting of 19 vacancies lying in the {111} plane of a f.c.c. lattice, and they got analogous results.

As we have pointed out, Vineyard's model permits one to simulate both cascades and structural defects. This makes it possible to treat the reactions of dynamic crowdions and focusons with different types of structural defects, which is very important for analyzing radiation damage at high doses. The authors of this review have utilized this possibility, and have treated the interaction of chains of atom-atom collisions with an interstitial atom and a vacancy in a b.c.c. lattice (α-Fe)[30] by applying the previously described modeling algorithm (see Chap. 3).

The defects were located in the region of passage of a dynamic crowdion. This is of great interest from the standpoint of the expected physical effects. In particu-

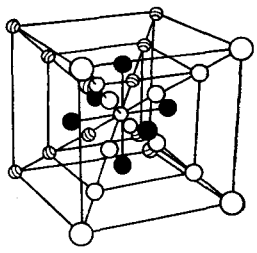

FIG. 22. The recombination region of a Frenkel' pair in α-Fe at 0 °K. A vacancy lies at the center of the cube. Interstitials lying at one of the 24 ⟨111⟩ positions (open spheres) or six of the ⟨100⟩ positions (solid spheres) will recombine with it.

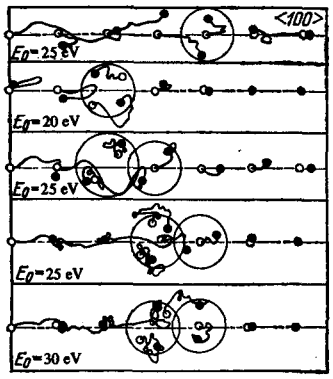

FIG. 23. Interaction of dynamic crowdions of different initial energies with an interstitial atom.[30] A dumbbell is lacking in the upper atomic chain. The motion of the atoms of the environment is not shown. $\theta_0 = 5°$.

lar, an interstitial atom was positioned in the microcrystallite in the form of a dumbbell configuration. The previously calculated equilibrium configuration, which includes the displacement of the atoms surrounding the dumbbell, was used as the initial conditions in the microcrystallite. The dumbbell was positioned at different distances from the first atom of the chain of collisions, as shown in Fig. 23. Several series of atomic collisions with different initial energies of the primary knock-on atom were calculated in such a perturbed atomic row.

As the modeling calculations showed, the reaction of a dynamic crowdion with a dumbbell strongly depends on the energy of the primary knock-on atom. Up to a certain threshold (the energy of the atom of the chain of collisions closest to the dumbbell being $E \approx 13$ eV), the chain of replacements is reflected from the dumbbell upon approaching it, and it ceases its forward movement, while spending the energy in shifting the dumbbell into a different plane (see Fig. 23). In this case, the dumbbell serves as a sort of shield, so that further energy transport along the chain to it practically ceases.

Above the stated threshold, the energy of the dynamic crowdion now suffices to pass by the dumbbell, most often by replacing one of its atoms and ejecting it into a neighboring cell. However, this also leads to stopping the dynamic crowdion and to forming a complex of two interstitial atoms (two dumbbells in neighboring cells). This configuration of the complex is metastable, and in time the complex transforms to the stabler configuration shown in Fig. 15.

The reactions with vacancies were calculated analogously. It was established that the reaction of a dynamic crowdion with a vacancy is also energy-dependent. Up to a certain energy threshold (with the energy of the atom of the chain closest to the vacancy $E \approx 1.5$ eV), a dynamic crowdion approaching a vacancy (Fig. 24) cannot pass it, but ceases its forward motion by annihilating with it.

If we compare the crystal containing a vacancy before and after passage of a dynamic crowdion, we conclude that the main result of this reaction proves actually to be a shift of the vacancy from its original site to a site corresponding to the origin of the chain of collisions. Thus, the crowdion transfers the vacancy in a very short time for a distance of several lattice constants.

With increasing energy, a dynamic crowdion can pass a vacancy without collapsing it, and it continues its forward motion. In this case, for the same initial energy of the primary knock-on atom, a dumbbell interstitial is produced one interatomic distance farther than in the case without the vacancy (the latter has been confirmed also by Mikhlin and Nelaev for copper[92]). Here, if the vacancy originally lies near the origin of the chain, then a complex of two vacancies is produced. Naturally, cases in which a dynamic crowdion passes a vacancy but does not carry the interstitial outside the bounds of its spontaneous-annihilation zone reduce to the first type of reaction.

Model calculations have been performed subsequently on the reactions of dynamic crowdions with twin boundaries, heavy impurities[93] and precipitates of a second phase.[94] In the first case, one "observed" stopping of the dynamic crowdions at the obstacle defect, and precipitation of the interstitial atoms. This recalled the above-discussed reactions of interaction of dynamic crowdions with interstitial atoms. In the cited cases (of an interstitial atom, a twin boundary, and a heavy impurity), one observes a seeming decoration of the stated defects by the interstitial atoms.

In the case of precipitates of a second phase (here reactions of crowdions with Guinier–Preston zones were treated; see[94]), they were noted to dissolve during irradiation owing to transport of the material of the second phase by the dynamic crowdions. The latter has also been found in reactor experiment.[94]

We have taken up above only the fundamental results and lines of study of defects and their interactions. This field of machine modeling is currently represented by a voluminous literature to which we shall refer the reader (vacancies,[6,72,95–99] interstitials,[6,74,99,100] impurities,[7,99,101–103] dislocations,[104–116] free surfaces,[99] pores,[99] precipitates,[7,99,101–103] antiphase domains and antiphase boundaries,[50,117] here we are always referring to static interaction of defects).

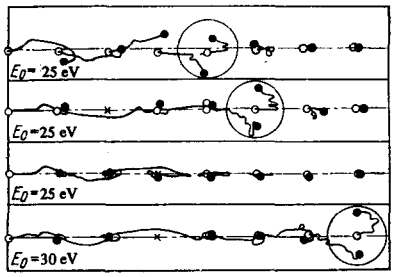

FIG. 24. Interaction of dynamic crowdions of different initial energies with a vacancy (×).[30] A vacancy is lacking in the upper atomic chain. The motion of the atoms of the environment is not shown. $\theta_0 = 5°$.

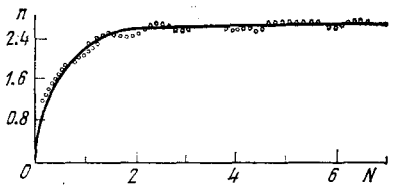

FIG. 25. Concentration of the remaining defects n as a function of the irradiation dose.[121]

5. MODELING OF ANNEALING PROCESSES

The "embryonic" spatial and size distributions of the defects left at the site of passage of collision cascades are significantly altered in time by annealing processes. Cascades of collisions are continuously being initiated in the irradiated material during irradiation. The existing defect distribution is simultaneously annealed by both thermal and radiation-stimulated driving forces.

When we take account of the latter, it is convenient in simulating annealing processes to classify them (as is done in most studies) into radiation and thermal annealing. As we know, the former leads in low-temperature irradiation to saturation in the change in properties of the irradiated material with increasing dose. Thermal annealing is caused by thermally-activated interaction of defects. Hence it is especially important at higher temperatures.

A. Radiation annealing

Cooper, Koehler, and Marx[118] were the first to note radiation annealing in experiments with deuteron irradiation of noble metals at 10 °K. They proposed the following relationship for the effective rate of change of the concentration of Frenkel' pairs (the number of Frenkel' pairs per lattice atom):

$$\frac{dn}{dt} = J_0(1-\beta n), \tag{9}$$

Here J_0 is the rate of production of defects (Frenkel' pairs) caused by the bombardment, and βJ_0 is the probability that an existing Frenkel' pair will annihilate with any other pair. If we assume J_0 and β to be constants in the given relationship, then

$$n = \frac{1}{\beta}[1-\exp(-J_0\beta t)]. \tag{10}$$

This means that a certain saturation concentration $n_{max} = 1/\beta$ of Frenkel' defects should exist. Radiation annealing is explained by spontaneous (rather than thermally-activated) recombination of vacancies and interstitial atoms; they mutually annihilate if the distance between them falls below a certain critical value. If we start with the existence of such a spontaneous-recombination region (see Chap. 4), then we must know how to relate the quantity β specifically to it.

Lück and Sizmann[119] have related the quantity β to the size of the spontaneous-recombination region as follows for the case of electron irradiation in which individual Frenkel' pairs are created. When all the vacancies and interstitial atoms produced by the bombarding flux lie far enough apart, the total concentration of unstable sites in the lattice is the sum of the quantities $i\alpha_0$ (i is the number of interstitial atoms per lattice atom and α_0 is the volume of the spontaneous-recombination region) and $v\alpha_0$ (v is the number of vacancies per lattice atom). Actually, however, certain vacancies lie so close to one another that their spontaneous-recombination regions overlap.

The same is true of interstitial atoms. Thus the quantity α_0 must be replaced by the function $\alpha(v, i)$, which declines with increasing defect concentration. In order to determine this function, in[119-121] they used machine-modeling methods in which the recombination was determined in a highly simplified way as compared with the way that we mentioned in Chap. 4. Namely, they assumed that the recombination region has the shape of a cube whose edge is six interatomic distances ($\alpha_0 = 7^3 = 343$). The calculations of the annealing process were made in a microcrystallite that was a three-dimensional cubic lattice with a number of atoms equal to 10^3.

They first used a random-number generator to find the spatial coordinates of the vacancies (the total number of them is determined by the chosen dose). Then stable Frenkel' pairs were generated. That is, the coordinates of the corresponding interstitials were found in the same way. They assumed here that the vacancy-interstitial distance of each stable primary Frenkel' pair is random, and that it varies over the range of 4–21 lattice periods. Thus, they did not take account of the primary unstable Frenkel' pairs for which the vacancy-interstitial distance lay within α_0.

If a newly created interstitial fell within the recombination region of an already-existing vacancy as they increased the number of Frenkel' pairs in the studied coordinate volume, then they assumed the corresponding defects to have recombined. Figure 25 shows the dose-dependence of the number of "surviving" Frenkel' pairs as obtained by the above-stated method. The plotted coordinates are: N, the total number of initially produced Frenkel' pairs (the value of N is proportional to the irradiation dose), and n, the remaining fraction of the Frenkel' defects that have "survived" after radiation annealing. For irradiation at a constant dose rate, $N = at$, where $a = \text{const}$.

By assuming that the relationship $n = n(N)$ found by the machine-modeling method (see Fig. 25) satisfies Eq. (10), Lück and Sizmann found the corresponding function $\alpha = \alpha(n)$ (Fig. 26). The results of the calculations for α can be represented in the form

$$\alpha/\alpha_0 = 1 - 0.47\alpha_0 n \qquad (\alpha_0 n \ll 1). \tag{11}$$

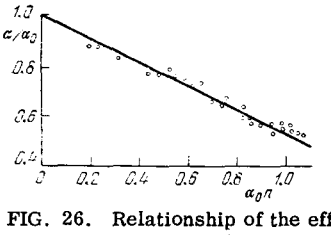

FIG. 26. Relationship of the effective size of the spontaneous-combination region α/α_0 to the defect concentration.[121]

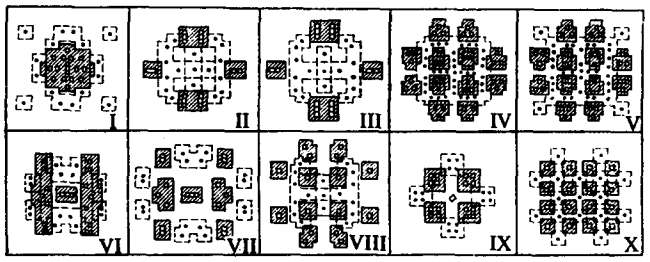

FIG. 27. The post-cascade structures (before radiation annealing) that were used for the modeling calculations. The diagrams show the structure of the cascades in gold (I—III), copper (IV—IX), and aluminum (X), according to Jan's calculations. The structures range from heterogeneous (I) to homogeneous (X). ●—interstitial, □—vacancy; the recombination zones are outlined.

The use of this relationship found in the machine calculations is corroborated by the experimental results of Balarin and Hauser.[122]

An analogous method was used in[123] to study radiation annealing in neutron irradiation. Whereas we can assume that mainly Frenkel' pairs are produced in electron irradiation, we must also take account in neutron irradiation of more complex defect structures, and of their geometry and distribution, as formed after passage of cascades of collisions. In their model, Lück, Bradatsch, and Sizmann[123] took account of the features of the defect structure found by Jan[124-125] that occur after passage of a single cascade.

According to Jan, in isolated cascades the vacancies are distributed over a smaller volume than the interstitials. This distribution of the different types of defects is more marked for the more rigid interatomic interaction potentials. Therefore different post-cascade structures are typical of different metals (Fig. 27). For example, the post-cascade structures (for a single cascade) in gold and aluminum differ very greatly: it is a homogeneous mixture of vacancies in aluminum, while in gold the interstitials lie around grouped vacancies.

While the radiation annealing arose in electron irradiation by overlap of Frenkel' pairs, in neutron irradiation, the computer permits one to treat the defect structures that survive after overlap of various post-cascade structures.[6)] Here one can reveal the effect of the type of post-cascade structures on the results of radiation annealing. The obtained results pictorially demonstrate the effect of post-cascade "primer" structures on the overall distribution of defects after annealing. Figure 28 gives one of the examples of this effect. Since the post-cascade structures (before annealing) differ in aluminum and gold (see Fig. 27), the consequences of radiation annealing also prove to differ. Namely, for a given irradiation dose, the defect distributions after annealing in the bulk of the crystal for Al and Au prove to differ qualitatively (homogeneous for Al, but a heterogeneous defect distribution for Au).

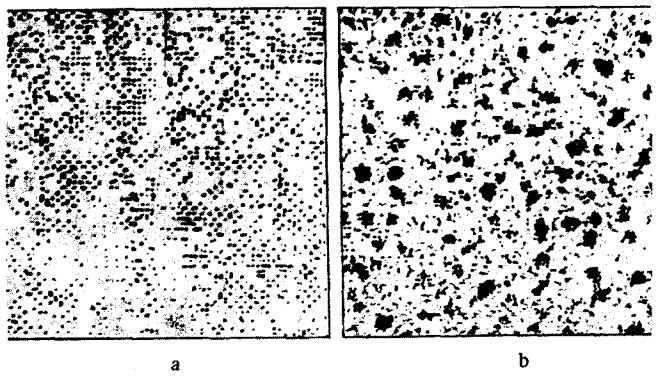

FIG. 28. The pattern of distribution of defects at a dose $\alpha_0 N = 5.31$ and a defect concentration $\alpha_0 n = 1.47$ for an Al cascade (a) and an Au cascade (b). The dark circles are vacancies, and the light ones are interstitials.

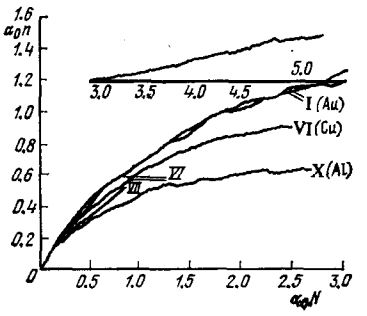

FIG. 29. Dose-dependence for certain post-cascade structures (see Fig. 27). Two calculations each have been performed for the cascades I and VI.

The dose-dependences of the concentration of surviving defects also proved to be sensitive to the post-cascade structure (Fig. 29). This indicates that the numerous deviations in the dose-dependences of the properties of irradiated specimens of different materials arise at least partly from the differing structures of the post-cascade damage in them.

B. Thermal annealing

Beeler[50] has proposed a computer model that simulates thermal annealing of "embryonic" radiation damage. Beeler's model assumed that one knows the activation energy for migration of different types of defects, with account taken of their mutual interactions. Generally these data can be obtained independently (see, e.g., Chap. 4) by using the computer-modeling methods discussed above. Different types of defects have different activation energies, and therefore, different mean migration times.

In Beeler's model in the average-jumping-time approximation, the computer traces the evolution of an "embryonic" defect distribution that is adopted at the initial instant of time, while taking consideration of the possibility of their random walk, combination, and

[6)] One of the mechanisms of radiation annealing is the capture of a crowdion by a vacancy cluster. This mechanism has been treated analytically by one of the present authors and Mikhlin[126] in connection with studying the dependence of the critical shear stress on the integral dose of fast neutrons. The same article treated the kinetics of growth of clusters consisting of interstitial atoms arising from crowdion capture.

TABLE 12. Block diagram of the algorithm modeling thermal annealing.

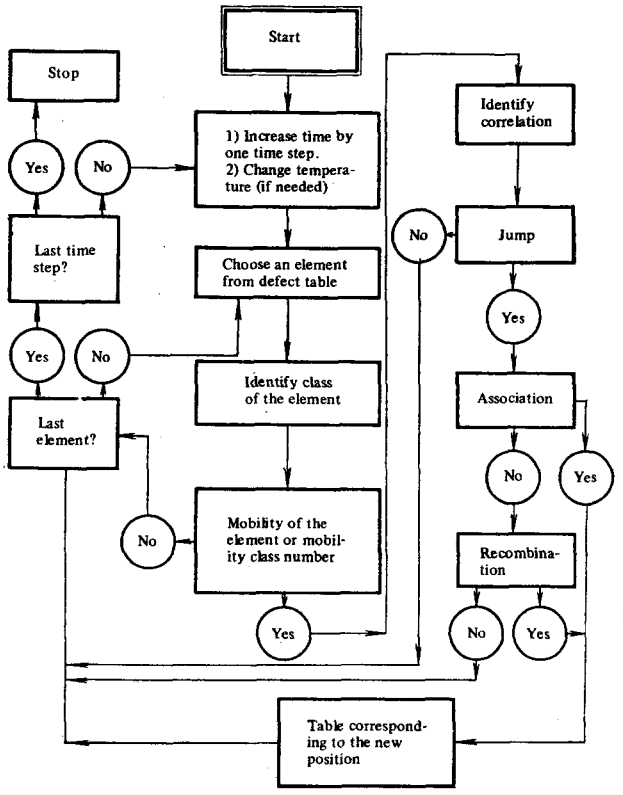

breakdown (a random-number generator governs the choice of a defect from the ensemble and the direction in which it jumps throughout the annealing time.) Table 12 gives the overall block diagram of Beeler's algorithm that models thermal annealing of post-cascade structures.

Before we discuss the results that Beeler got, we note that the activation energies for migration of interstitials are severalfold smaller for many metals and alloys than those for migration of vacancies. Hence, we can consider the vacancies to be immobile over a broad temperature range in the first stage of annealing, while the interstitials can collect into clusters. In this temperature range, the primary defect structure rather quickly converts into collected clusters of interstitial atoms in a field of relatively stationary solitary vacancies and divacancies and stationary larger vacancy clusters. Here the size distribution of the vacancy clusters remains close to their initial distribution. If the cascade had produced large vacancy clusters, then about 42% of the defects initially produced, according to Beeler's data,[50] withstand the simulated short-term thermal annealing.

In the case in which large vacancy clusters do not remain after passage of a cascade, only 30% of the defects produced by the cascade withstand short-term annealing. By definition, the process of short-term annealing lasts until all the interstitials have collected into immobile clusters. For example, in α-Fe this takes about 200 jumps per interstitial (about one microsecond). Figure 30 shows a graph of the continuous decline in the fraction of the interstitial atoms in mobile configurations during short-term annealing.

According to Beeler, the process of long-term annealing follows the short-term process, and it depends mainly on migration of vacancies, since actually all of the interstitials prove to be already collected into immobile clusters. Collisions between the mobile vacancy configurations and small clusters of interstitials lead again to appearance of mobile interstitials. For example, collisions of divacancies and vacancies with tri-interstitials lead to appearance of single interstitials and bi-interstitials. The ratio of the rates of annihilation and cluster formation in long-term annealing does not differ from that in short-term annealing.

According to Beeler, about 58% of the annihilations and 42% of the cluster formations occur during short-term annealing in the case of "embryonic" damage with large vacancy clusters. If we adopt this same relationship for long-term annealing, then, since only 42% of the defects endure short-term annealing, about 18% of the defects produced in the cascades must endure both stages of annealing. We can expect analogously that about 9% of the defects of the initially produced "embryonic" damage not containing large vacancy clusters will survive both the short- and the long-term annealing.

Absolutely, thermal annealing plays a very important role in the development of radiation damage of crystals. This fact makes it very topical to design further machine experiments within the framework of Beeler's model or generalizations of it (see also[138,139]). The application of this model is currently limited to only very simple post-cascade structures, owing to lack of information on the mutual interaction of defects of complex structure.

6. COMPUTER SIMULATION OF THE ALTERATION IN PROPERTIES OF IRRADIATED SPECIMENS

Above we have discussed the currently known models of computer simulation of radiation defects, which permit us to find in some approximation the types of defect structures that arise under the influence of the hard radiation of nuclear particles. However, evidently the finding of the defect structures, i.e., finding the spatial distributions of different types of crystal-lattice defects, is only the first step of study. The stage that follows it must consist in studying the effect of the entire set of defects on the alteration of various physical properties of solids upon irradiation.

It turns out that computer-simulation methods may prove very useful at this stage of study also. However, there is currently only one example of such a simulation that permitted getting an entire set of interesting physical results. We refer to the line of studies

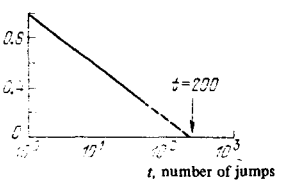

FIG. 30. The results of modeling of annealing. The ordinate represents the fraction of interstitials in mobile configurations. The results pertain to cascades of energies 5–20 keV in α-Fe.

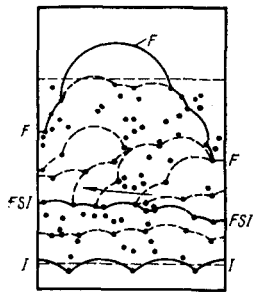

FIG. 31. Movement of a dislocation through a configuration of 100 obstacles at a breakaway angle of 130°. The initial (*I*) and final (*F*) positions and the position at the final stress increase (*FSI*) are given. The dotted lines indicate the intermediate positions.

started by Foreman and Makin.[127-129] These studies proposed a methodology of computer experimentation that models the migration of dislocations through an arbitrary set of obstacles. As we know, obstacles of this type for dislocations are point defects, dislocation loops, clusters, etc. The discussed method permits one to determine the effect of irradiation (i.e., the effect of the entire set of lattice defects) on the alteration of the critical shear stress in irradiated specimens.

A. The procedure of modeling movement of dislocations in a crystal defect and the fundamental results

As we know, hardening in metals and alloys involves the resistance exerted by different types of obstacles to the movement of dislocations. In many cases, the obstacle defect interacts locally with the slipping dislocation. Hence a treatment of the obstacle as a "point barrier" can be a good approximation. The essence of the method of computer modeling discussed here consists in the following. First one obtains a random defect distribution in the slip plane of the dislocation by using a random-number generator. Generally one assumes here that these defects can differ both in their nature and in size.

Depending on the program stored in the computer, a dislocation moves freely under the influence of the applied stress only until some obstacle appears along its path. The dislocation becomes pinned to the obstacle, and bends outward between adjacent pairs of defects. Here the program takes account of the fact that pinning does not arise for those defects that have an angle between the shoulders of the dislocation at the obstacle (Φ) at the given stress less than the critical angle (Φ_c) (each type of defect has its own critical angle). Then the dislocation breaks free from the obstacle.

The critical angles Φ_c for different types of defects in this model are assumed to be known. Evidently $\Phi_c \to \pi$ for very weak defects, whereas $\Phi_c \to 0$ for infinitely strong defects. Generally one can find the value $0 < \Phi_c < \pi$ by a special examination of the interaction of some particular defect with a dislocation.

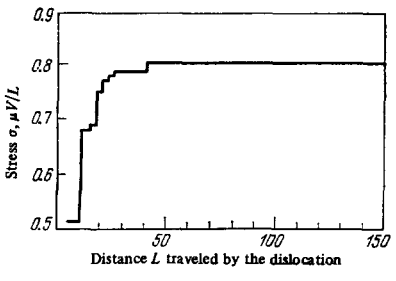

FIG. 32. A typical stress variation as a dislocation penetrates an arbitrary configuration of barriers of width 100 *L* (breakaway angle 10°).

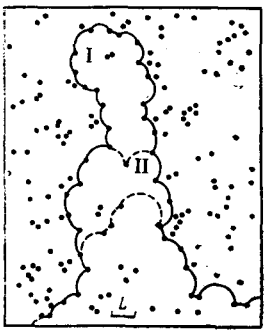

FIG. 33. A dislocation that uses the easy path of movement through an arbitrary configuration of strong obstacles (breakaway angle 10°). Removing the obstacles I and II would permit the dislocation to penetrate farther into the arrangement of barriers.

As the applied stress is increased (in the discussed machine experiments, the stress σ took on a discrete sequence of increasing values), the dislocation migrates until it manages to pass the entire set of barriers (Fig. 31). Naturally, each value here of the applied stress corresponds to a quite definite distance traversed by the dislocation. Figure 32 shows the corresponding functional relationship. The maximum value of the applied stress at which the dislocation passes by the entire set of obstacles is taken to be the critical shear stress. Foreman and Makin's computer experiments permit one to determine the relationship between this critical stress and the type of lattice disturbance.

Whenever the dislocation encounters powerful enough obstacles ($\Phi_c \leq 10°$), it uses for its progress local windows in the pattern of barriers ("weak" points). When such a window exists, the dislocation breaks through the pattern of barriers, as is shown in Fig. 33. During such a breakthrough, the rest of the dislocation remains immobile. However, loops are formed around small groups of strong obstacles.

The dislocation line remains relatively straight for weak barriers for which $\Phi_c \geq 160°$, since it takes a small force to overcome the resistance. Then loops are not formed, while the results of the modeling agree with Friedel's theory.[140] A mixture of obstacles of different strengths is treated in[128].

Foreman[129] has also applied the above-described modeling method to the problem of loop hardening in f.c.c. crystals. He was the first to calculate in detail the motion of a slipping dislocation through an arbitrary arrangement of dislocation loops. The critical shear stress that he found for the loop hardening proved to have the form

$$\sigma_c = \frac{1}{4}\mu B \sqrt{N}\, d, \qquad (12)$$

Here N in the bulk density of all the loops, d is the diameter of a loop, μ is the shear modulus, and B is the Burgers vector. The latter calculation is especially important for studying the consequences of radiation damage in which the defect clusters are transformed

TABLE 13. Structure of the system modeling the effect of irradiation on mechanical properties.

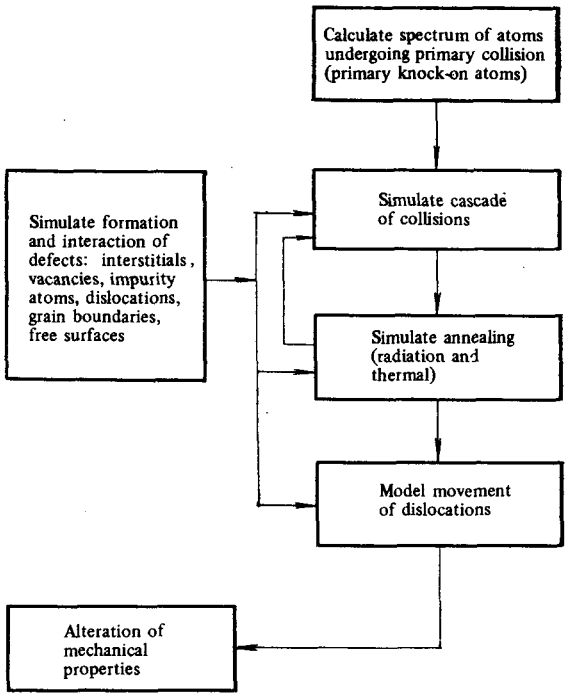

into dislocation loops as association proceeds (see Chap. 4). Along this line, the study of Predvoditelev and Nichugovskiĭ[130] is of interest. They studied the movement of a dislocation through a dislocation "forest" within the framework of the machine model of Foreman and Makin.

B. Modeling of thermoactivated movement of dislocations past an obstacle

Foreman and Makin's results apply only to the low-temperature region, where one can neglect thermoactivated overcoming of obstacles by moving dislocations. A logical continuation of these studies is the machine model of Zaĭtsev and Nadgornyĭ.[131] Within the framework of the machine model of Foreman and Makin, these authors proposed also taking account of the thermoactivated release of dislocations from a defect, even when $\Phi > \Phi_c$. They determined the probability of such a thermoactivated process by the Monte Carlo method. Here they treated the corresponding expected site and time of activation as random quantities.

Calculations using this model are yet just beginning. It has been established that the nature of the movement of dislocations depends substantially on the temperature. Evidently, the rate of loading must affect the results of these calculations, since the thermoactivated release of dislocations cannot be substantial with sufficiently rapid loading.

7. CONCLUDING REMARKS, PROSPECTIVES

The further development of computer experiments faces an entire set of problems. We have discussed many of them above. Here we would like to emphasize again the vast importance of further analysis of the atom-atom interaction potentials for the development of computer modeling of radiation damage. Namely, the lack here of the needed data hinders obtaining results in crystals more complicated that simple cubic metals. For example, it is not now clear how one should model radiation defects in covalent crystals, in which the ejection of an atom from its site necessarily entails a substantial change in its electronic structure.

However, if we digress from the problem of atom-atom potentials, or, e.g., treat media in which these potentials are know, then the immediate future of the development of computer modeling of radiation damage should involve development of complicated modeling systems which will incorporate the various more special algorithms, many of which we have mentioned above.

The problem of creating this type of system was first discussed in 1969 at the Vienna symposium on radiation damage.[132] They discussed there also the provisional structure of such a system (Table 13). One assumes that the calculation must start with finding the characteristics of the primary knock-on atom. Here the Monte Carlo method[133] is most convenient for carrying out the spectral calculations for the primary knock-on atom. If one knows the initial energy of the primary knock-on atom and its direction of motion, one can model the cascade of collisions by using one of the algorithms of Chap. 3.

One must choose the needed algorithm with account taken of the temperature of the irradiated specimen, and the prehistory of the region where the cascade occurs. The configurations of the defects of the "embryonic" damage must be calculated by using the algorithms described in Chap. 4. The primary defect distribution remaining after a cascade has passed must be introduced directly as the initial conditions in the algorithm for short-term, and then for long-term annealing (Chap. 5).

The algorithms of Chap. 6 will relate the new structure to the alteration of properties. One can accelerate such a combined calculation by prior preparation of a library of atomic configurations of defects with their fundamental characteristics. Moreover, one can try in an individual crystal in the case of non-interacting cascades to prepare a library of cascades for the set of initial directions and energies of the primary knock-on atom.

Realization of such a system of algorithms requires the most powerful computers. The further development and perfection of the system itself depends in many ways on the progress of computing technology. Thus, one of the possible paths of development of machine modeling of radiation damage could even be the invention of a specialized computer. Such projects as applied to other problems of many interacting particles are already being discussed (e.g., Schee, Veltman, Speet, and de Haan have proposed the scheme of a processor for calculations using Yang's algorithm within the framework of the Ising model[134]).

We emphasize in concluding that many of the above-discussed methods can be successfully used for solving

also problems of solid-state physics not involving radiation damage. Among them we mention, e.g., certain problems of diffusion of impurities in crystals and their capture in traps, "tube" diffusion of impurities along dislocations, diffusion and cluster formation of long-lived quasiparticles (e.g., excitons), etc.

Naturally, one can extend the list of this sort of problems.

The authors sincerely thank for unforgettable stimulating discussions É. L. Andronikashvili, on whose initiative this review was written, and A. N. Orlov, who examined the manuscript of this review, for an entire series of useful advice.

[1]J. B. Gibson, A. M. Goland, and M. Milgram, G. H. Vineyard, Phys. Rev. 120, 1229 (1960).
[2]J. R. Beeler, *ibid.* 150, 470 (1966).
[3]C. Erginsoy, G. H. Vineyard, and A. Englert, *ibid.* A133, 595 (1964).
[4]C. Erginsoy, G. H. Vineyard, and A. Shimizu, *ibid.* A139, 118 (1965).
[5]R. A. Johnson, *ibid.* 145, 423 (1966).
[6]R. A. Johnson, *ibid.* A134, 1329 (1964).
[7]R. A. Johnson, G. J. Dienes, and A. C. Damask, Acta Met. 12, 1215 (1964).
[8]T. L. Gilbert and A. C. Wahl, J. Chem. Phys. 47, 3425 (1967).
[9]D. E. Rimmer and A. H. Cottrell, Phil. Mag. 2, 1345 (1957).
[10]G. H. Vineyard, transl. in Fizika kristallov s defektami (Physics of Crystals with Defects), Vol. 3, Tbilisi, Institute of Physics of the Academy of Sciences of the Georgian SSR, 1966, p. 5.
[11]M. W. Thompson, Defects and Radiation Damage in Metals, Cambridge Univ. Press, 1969 (Russ. Transl, Mir, M., 1971).
[12]G. H. Vineyard, Phys. Rev. 120, 1229 (1960).
[13]W. A. Harrison and F. Seitz, Phys. Rev. A98, 1530 (1955).
[14]W. S. Snyder and J. Neufeld, *ibid.* 97, 1636 (1955); 99, 1326 (1955); 103, 862 (1956).
[15]G. H. Kinshin, R. S. Pease, Rept. Progr. Phys. 18, 1 (1955).
[16]G. J. Dienes, G. H. Vineyard, Radiation Effects in Solids, N.Y., Interscience Publishers, Inc., 1957 (Russ. Transl., IL, M., 1960).
[17]F. Seitz and J. S. Koehler, Sol. State Phys. 2, 307 (1956).
[18]J. A. Brinkman, J. Appl. Phys. 25, 961 (1954).
[19]A. Seeger, in: Proc. of 2nd Intern. Conference of Peaceful Uses of Atomic Energy, v. 6, Geneva, 1958, p. 250.
[20]D. K. Holmes, see Ref. 10, Vol. 3, p. 51.
[21]A. N. Orlov, in Deĭstvie yadernykh izlucheniĭ na materialy (Action of Nuclear Radiations on Materials), Izd-vo AN SSSR, M., 1962, p. 288.
[22]A. Larsen, Brookhaven Nat. Lab. Report 7979.
[23]V. V. Kirsanov and Z. Ya. Osipova, Dinamika radiatsionnogo povrezhdeniya pri gipoteticheskom 0°K (sbornik programm 1) (Dynamics of Radiation Damage At Absolute Zero (Collection of Programs 1). Preprint of the Scientific Research Institute of Atomic Reactors P-145, Melekess, 1972.
[24]G. H. Vineyard and C. Erginsoy, in: Proc of Conference on Crystal Lattice Defects, Kyoto, Japan, 1962, p. 189.
[25]G. H. Vineyard, J. Phys. Soc. Japan 18, Suppl. 3, 144 (1963).
[26]V. I. Klimenkov, V. V. Kirsanov, and Z. Ya. Osipova, Atomnaya Énergiya 23, 356 (1967) [Sov. Atomic Energy 23, 1109 (1967)].
[27]V. I. Klimenkov, V. V. Kirsanov, and Z. Ya. Osipova, Abstracts of Reports of the Interuniversity Conference on Problems of Radiation Physics, Tomsk Univ. Press, 1967, p. 82.
[28]V. I. Klimenkov, V. V. Kirsanov, and Z. Ya. Osipova, Kristallografiya 13, 1060 (1968) [Sov. Phys.-Cryst. 13, 922 (1969)].
[29]V. V. Kirsanov, in Radiatsionnaya fizika tverdogo tela i reaktornoe materialovedenie (Radiation Solid State Physics and Reactor Materials Science), Atomizdat, M., 1970, p. 27.
[30]V. M. Agranovich and V. V. Kirsanov, Fiz. Tverd. Tela 13, 3373 (1971) [Sov. Phys.-Solid State 13, 2833 (1972)].
[31]A. H. Domingos, A Theoretical Study of Radiation Damage in Aluminium. Ph. D. thesis (University of Washington, 1963), p. 109 (Ref. "Dissert. Abstr." 25 (2), 1097 (1964)).
[32]J. N. Lomer and M. Pepper, Phil. Mag. 16, 1119 (1967).
[33]R. Nelson, M. Thompson, and H. Montgomery, *ibid.* 7, 1385 (1962).
[34]J. Sanders and J. Fluit, Physica 30, 129 (1964).
[35]T. S. Pugacheva, Fiz. Tverd. Tela 9, 102 (1967) [Sov. Phys.-Solid State 9, 75 (1967)].
[36]S. T. Konobeevskiĭ, Deĭstvie oblucheniya na materialy (Action of Irradiation on Materials), Atomizdat, M., 1967.
[37]V. M. Agranovich and V. V. Kirsanov, Fiz. Tverd. Tela 11, 674 (1969) [Sov. Phys.-Solid State 11, 540 (1969)].
[38]L. Van Hove, Phys. Rev. 95, 249 (1954).
[39]V. F. Turchin, Medlennye neĭtrony (Slow Neutrons), Gosatomizdat, M., 1963 (Engl. Transl., Israel Program for Scientific Translations, Jerusalem, 1965).
[40]V. M. Agranovich and V. V. Kirsanov, Fiz. Tverd. Tela 12, 2671 (1970) [Sov. Phys.-Solid State 12, 2147 (1971)].
[41]J. R. Beeler, Jr., J. Appl. Phys. 35, 2226 (1964).
[42]J. R. Beeler and D. G. Besco, in: Radiation Damage in Solids, v. 1, Vienna, IAEA, 1962, p. 43.
[43]J. R. Beeler and D. G. Besco, J. Phys. Soc. Japan 18, Suppl. 3, 159 (1963).
[44]J. R. Beeler and D. G. Besco, J. Appl. Phys. 34, 2873 (1963).
[45]J. R. Beeler and D. G. Besco, Phys. Rev. A134, 530 (1964).
[46]J. R. Beeler, J. Nucl. Mat. 15, 1 (1965).
[47]M. Ioshida, J. Phys. Soc. Japan 16, 44 (1961).
[48]M. T. Robinson and O. S. Oen, Phys. Rev. 132, 2385 (1963).
[49]R. A. Johnson, in: Diffusion in Body-centered, Cubic Metals, Cleveland, ASM, Ohio, ASB, 1965, p. 375 (Russ. Transl., "Metallurgiya," M., 1969, p. 357).
[50]J. R. Beeler, in: Symposium on Radiation Damage in Reactor Materials, v. 2, Vienna, IAEA, 1969, SM-120/E-1.
[51]M. J. Attardo and J. M. Galligan, Phys. Rev. Lett. 17, 191 (1966). P. Petroff and J. Washburn, in: Intern. Conference on Vacancies and Interstitials in Metals, v. 2, Kernforschungsanlage, Jülich, Germany, 1968, p. 485. Eds. A. Seeger *et al.*, Wiley, New York, 1970.
[52]V. M. Agranovich and É. Ya. Mikhlin, Atomnaya Energiya 12, 385 (1962); V. M. Agranovich, É. Ya. Mikhlin, and L. P. Semenov, *ibid.* 15, 393, 404 (1963); [Sov. Atomic Energy 12, 410 (1962); 15, 1140, 1155 (1963)], *ibid.* 15, 400 (1963).
[53]E. P. Wigner, J. Appl. Phys. 17, 857 (1946).
[54]D. E. Thomas, in: Nuclear Metallurgy v. 3, N.Y., Amer. Inst. of Min. Met. and Petrol Eng., N.Y., 1956, S.R., N 3. L. R. Aronin, J. Appl. Phys. 25, 344 (1954).
[55]L. T. Chadderton, D. V. Morgan, and I. Torrens, Phys. Lett. 20 (4), 4 (1966).
[56]I. Torrens and L. T. Chadderton, Phys. Rev. 159, 671 (1967).
[57]R. O. Jackson, H. P. Leighly, and J. D. R. Edwards, Phil. Mag. 25, 1169 (1972).
[58]J. J. O. Varley, Nature 174, 886 (1954).
[59]B. L. Eyre, J. Phys. F3, 422 (1973).
[60]M. Rühle, Phys. Stat. Sol. 19, 263 (1967).
[61]M. Rühle, in: Radiation Damage in Reactor Materials, v. 1, Vienna, IAEA, 1965, p. 113.
[62]G. Thomas, Transmission Electron Microscopy of Metals, N.Y., Wiley, 1962 (Russ. Transl., IL, M., 1963).
[63]E. W. Müller, J. Appl. Phys. 27, 474 (1956).

[64]E. W. Müller, Adv. Electronics Electron Phys. 13, 83 (1960) (Russ. Transl., Usp. Fiz. Nauk 77, 481 (1962)).
[65]E. W. Müller, Science 149, 591 (1965) (Russ. Transl., Usp. Fiz. Nauk 92, 291 (1967)).
[66]A. L. Suvorov, Usp. Fiz. Nauk 101, 21 (1970) [Sov. Phys.-Uspekhi 13, 317 (1970)].
[67]K. L. Merkle, see Ref. 61, Vol. 1, 1969, p. 159.
[68]V. V. Kirsanov, Kompleksy tochechnykh defektov v obluchennykh kubicheskikh metallakh, raspredelenie ikh po razmeram (Complexes of Point Defects in Irradiated Cubic Metals, and Their Size Distribution). Preprint of the Scientific Research Institute of Atomic Reactors P-60, Melekess, 1969.
[69]M. J. Makin, A. D. Whapham, and F. J. Minter, Phil. Mag. 7, 285 (1962).
[70]K. L. Merkle, in: Proc. of Symposium on the Nature of Small Defect Clusters, Ed. M. J. Makin, AERE-R 5269, Harwell, England, 1966, p. 8.
[71]R. P. Tucker, S. M. Ohr, and M. S. Wechsler, see Ref. 61, Vol. 1, 1969, p. 132.
[72]R. A. Johnson and E. Brown, Phys. Rev. 127, 446 (1962).
[73]R. A. Johnson, J. Phys. Chem. Sol. 26, 75 (1965).
[74]R. A. Johnson, Phys. Lett. 19, 191 (1965).
[75]H. B. Huntington and F. Seitz, Phys. Rev. 61, 315, 324 (1942).
[76]J. D. Eshelby, J. Appl. Phys. 25, 255 (1954).
[77]I. Tewordt, Phys. Rev. 109, 61 (1958).
[78]A. Seeger and E. Mann, J. Phys. Chem. Sol. 12, 326 (1960).
[79]V. I. Klimenkov, V. V. Kirsanov, and Z. Ya. Osipova, in Trudy mezhvuzovskoĭ konferentsii po radiatsionnoĭ fizike (Proceedings of the Interuniversity Conference on Radiation Physics), Izd. Tomskogo un-ta, Tomsk, 1970, p. 55.
[80]V. V. Kirsanov and Z. Ya. Osipova, Modelirovanie struckturnykh defektov i protsessov dinamiki radiatsionnogo povrezhdeniya v kristalle s defektami (sbornik programm 3) (Modeling of Structural Defects and Processes of the Dynamics of Radiation Damage in a Crystal with Defects (Collection of Programs 3)). Preprint of the Scientific Research Institute of Atomic Reactors P-147, Melekess, 1972.
[81]G. H. Vineyard, Disc. Farad. Soc., No. 31, 7 (1961).
[82]J. R. Beeler, Jr., see Ref. 70, p. 173.
[83]A. Seeger and D. Schumacher, in: Lattice Defects in Quenched Metals, Ed. R. M. J. Cotterill and M. Doyama *et al.*, N.Y., Academic Press, 1965, p. 15.
[84]A. Seeger, in: Proc. of Symposium on Irradiation in Solids and Reactor Materials, Vienna, IAEA, 1962, p. 67.
[85]R. Bullough and R. C. Perrin, Proc. Roy. Soc. A305, 541 (1968).
[86]M. E. Downey and B. L. Eyre, Phil. Mag. 11, 53 (1965).
[87]B. L. Eyre and A. F. Bartlett, *ibid.* 12, 261.
[88]R. D. Dokhner and A. N. Orlov, Izv. AN SSRS, ser. fiz. 31, 851 (1967).
[89]R. D. Dokhner and A. N. Orlov, FMM 25, 972 (1968) [Phys. Metals Metallogr. 25, No. 6, 13 (1968)].
[90]Yu. M. Plishkin and I. E. Podchinenov, FMM 32, 254 (1971). [Phys. Metals Metallogr. 32, No. 2, 29 (1972)].
[91]R. D. Dokhner, Fiz. Tverd. Tela 11, 1124 (1969) [Sov. Phys.-Solid State 11, 916 (1969)].
[92]É. Ya. Mikhlin and V. V. Nelaev, *ibid.* 14, 2153 (1972) [Sov. Phys.-Solid State 14, 1859 (1973)].
[93]V. V. Kirsanov, in Voprosy atomnoĭ nauki i tekhniki (Problems of Atomic Science and Technology), KhFTI-74-47, Khar'kov, FTI AN Ukr. SSR, 1974, 3.
[94]P. P. Grinchuk and V. V. Kirsanov, FMM 38, 756 (1974).
[95]R. A. Johnson, Phil. Mag. 16, 553 (1967).
[96]J. R. Beeler and R. A. Johnson, Phys. Rev. 156, 677 (1967).
[97]R. M. J. Cotterill and M. Doyama, see Ref. 83, p. 653.
[98]M. Doyama and R. M. J. Cotterill, Phys. Rev. A137, 994 (1965).
[99]J. R. Beeler, Jr., see Ref. 51, Vol. 2, p. 598.
[100]R. Perrin and R. Bullough, see Ref. 70, p. 43.
[101]R. A. Johnson and A. C. Damask, Acta Met. 12, 443 (1964).
[102]R. A. Johnson, *ibid.* 13, 1259 (1965).
[103]R. A. Johnson, *ibid.* 15, 513 (1967).
[104]R. Bullough and R. C. Perrin, AERE Report T. P. 292, Harwell, England, 1968.
[105]M. Doyama and R. M. J. Cotterill, in: Lattice Defects and Their Interaction, Ed. R. R. Hasiguti, N.Y., Gordon and Breach, 1967, p. 35.
[106]A. Englert and H. Tompa, J. Phys. Chem. Soc. 21, 306 (1961).
[107]A. Englert and H. Tompa, *ibid.* 24, 1145 (1965).
[108]M. Doyama and R. M. J. Cotterill, Phys. Lett. 13, 110 (1964).
[109]R. M. J. Cotterill and M. Doyama, Phys. Rev. 145, 465 (1966).
[110]M. Doyama and R. M. J. Cotterill, Phys. Lett. 14, 79 (1965).
[111]M. Doyama and R. M. J. Cotterill, Phys. Rev. 150, 448 (1966).
[112]R. Chang and L. J. Graham, Phys. Stat. Sol. 18, 99 (1966).
[113]P. C. Gehlen, A. R. Rosenfield and G. T. Hahn, Techn. Report No. 2 to the Office of Naval Research. Contract Nonr-5052 (00), NR 039-089.
[114]M. J. Norgett, R. C. Perrin, and E. J. Savino, J. Phys. F2, L73 (1972).
[115]P. C. Gehlen, R. G. Hoagland, and M. F. Kanninen, Scr. met. 6, 445 (1972).
[116]J. O. Schiffgens and K. E. Garrison, J. Appl. Phys. 43, 3240 (1972).
[117]J. R. Beeler, Jr., Phys. Rev. A138, 1259 (1965).
[118]H. G. Cooper, J. S. Koehler, and J. W. Marx, *ibid.* 97, 559 (1955).
[119]G. Lück and R. Sizmann, Phys. Stat. Sol. 5, 683 (1964).
[120]G. Lück and R. Sizmann, *ibid.* 6, 263.
[121]G. Lück and R. Sizmann, *ibid.* 14, K61 (1966).
[122]M. Balarin and O. Hauser, Phys. Stat. Sol. 10, 475 (1965).
[123]G. Lück, H. Bradatsch, and R. Sizmann, Nukleonik 8, 256 (1966).
[124]R. Jan, Phys. Stat. Sol. 6, 925 (1964).
[125]R. Jan, *ibid.* 7, 299; 8, 331.
[126]V. M. Agranovich and É. Ya. Mikhlin, Fiz. Tverd. Tela 9, 1089 (1967); 11, 1895 (1969) [Sov. Phys.-Solid State 9, 851 (1969); 11, 1527 (1970)].
[127]A. J. E. Foreman and M. J. Makin, Phil. Mag. 14, 911 (1966).
[128]A. J. E. Foreman and M. J. Makin, Can. J. Phys. 45, 511 (1967).
[129]A. J. E. Foreman, Phil. Mag. 17, 353 (1968).
[130]A. A. Predvoditelev and G. I. Nichugovskiĭ, Kristallografiya 17, 166 (1972) [Sov. Phys.-Cryst. 17, 132 (1972)].
[131]S. N. Zaĭtsev and É. M. Nadgornyĭ, Fiz. Tverd. Tela 15, 2669 (1973) [Sov. Phys.-Solid State 15, 1777 (1974)].
[132]J. R. Beeler, Jr., see Ref. 61, Vol. 1, 1969, p. 3.
[133]S. M. Ermakov, Metod Monte-Karlo i smezhnye voprosy (The Monte Carlo Method and Allied Problems), Nauka, M., 1971.
[134]E. v. d. Schee, B. P. Th. Veltman, L. Speet, and S. de Haan, Comput. Phys. Comm. 5, 104 (1973).
[135]R. E. Peierls, Transl. in: Teoreticheskaya fizika XX veka (Theoretical Physics of the 20th Century), IL, M., 1962, p. 165.
[136]V. M. Agranovich, see Ref. 10, Vol. 2, p. 247.
[137]V. M. Agranovich and N. M. Omel'yanovskaya, in Radiatsionnye i drugie defekty v tverdykh telakh (Radiation Defects and Other Defects in Solids), Vol. 1, Tbilisi, 1974, p. 240.
[138]D. G. Doran, Rad. Eff. 2, 249 (1970).
[139]J. M. Lanore, *ibid.* 22, 153 (1974).
[140]J. Friedel, Dislocations, Addison-Wesley, Reading, Mass., 1964 (Russ. Transl., Mir, M., 1967, Chap. 8, Sec. 4).

Translated by M. V. King